Circulation Research
JOURNAL OF THE AMERICAN HEART ASSOCIATION

Thyroid Hormone Targets Matrix Gla Protein Gene Associated With Vascular Smooth Muscle Calcification

Yoji Sato, Ryo Nakamura, Mitsutoshi Satoh, Kayoko Fujishita, Satoko Mori, Seiichi Ishida, Teruhide Yamaguchi, Kazuhide Inoue, Taku Nagao and Yasuo Ohno

Circ. Res. 2005;97;550-557; originally published online Aug 11, 2005;
DOI: 10.1161/01.RES.0000181431.04290.bd
Circulation Research is published by the American Heart Association. 7272 Greenville Avenue, Dallas, TX 72514
 Print ISSN: 0009-7330. Online ISSN: 1524-4571

Thyroid Hormone Targets Matrix Gla Protein Gene Associated With Vascular Smooth Muscle Calcification

Yoji Sato, Ryo Nakamura, Mitsutoshi Satoh, Kayoko Fujishita, Satoko Mori, Seiichi Ishida, Teruhide Yamaguchi, Kazuhide Inoue, Taku Nagao, Yasuo Ohno

Abstract—Thyroid hormones have marked cardiovascular effects in vivo. However, their direct effects on vascular smooth muscle cells have been unclear. Because thyroid hormones play critical roles in bone remodeling, we hypothesized that they are also associated with vascular smooth muscle calcification, one of the pathological features of vascular sclerosis. To test this hypothesis, we examined the effects of 3′,3,5-triiodo-L-thyronine (T_3) on the expression of calcification-associated genes in rat aortic smooth muscle cells (RAOSMCs). Quantitative RT-PCRs revealed that a physiological concentration of T_3 (15 pmol/L free T_3) increased mRNA level of matrix Gla protein (MGP), which acts as a potent inhibitor of vascular calcification in vivo, by 3-fold in RAOSMCs, as well as in cultured human coronary artery smooth muscle cells. In RAOSMCs transiently transfected with a luciferase reporter gene driven by the MGP promoter, T_3 significantly stimulated luciferase activity. In addition, RNA interference against thyroid hormone receptor-α gene diminished the effect of T_3 on MGP expression. Aortic smooth muscle tissues from methimazole-induced hypothyroid rats (400 mg/L drinking water; 4 weeks) also showed a 68% decrease in the MGP mRNA level, as well as a 33% increase in calcium content compared with that from the control euthyroid animals, whereas hyperthyroidism (0.2 mg T_3/kg IP; 10 days) upregulated MGP mRNA by 4.5-fold and reduced calcium content by 11%. Our findings suggest that a physiological concentration of thyroid hormone directly facilitates MGP gene expression in smooth muscle cells via thyroid hormone nuclear receptors, leading to prevention of vascular calcification in vivo. **(*Circ Res*. 2005;97:550-557.)**

Key Words: calcium ■ gene expression ■ nuclear receptors ■ vascular smooth muscle ■ thyroid hormone

Thyroid hormone has marked effects on differentiation, development, and metabolic balance of virtually every body tissue. The action of thyroid hormone is mediated by high-affinity thyroid hormone nuclear receptors (TRs), which recognize specific response elements in the promoters of target genes and regulate their transcriptional activity in response to the hormone. Alterations in thyroid hormone levels have a profound impact on the cardiovascular system, which include changes in myocardial contractility, heart rate, and resistance of peripheral vasculature. Hyperthyroidism leads to positive inotropic, lusitropic, and chronotropic effects on the heart and low systemic vascular resistance, whereas the opposite is observed in hypothyroidism. In myocardium, the mechanisms for these changes are based on altered expression levels of several key proteins involved in the regulation of intracellular ion homeostasis. The effects of thyroid hormone on cardiac contractility as well as rates of contraction and relaxation are mainly mediated by increases in the levels of the sarcoplasmic reticulum Ca^{2+}-ATPase and decreases in its inhibitor phospholamban in cardiomyocytes.[1] The positive chronotropic effect of thyroid hormone is associated with altered expression levels in plasmalemmal ion channels/transporters in the heart, such as Kv1.5, Kv4.2, minK, hyperpolarization-activated cyclic nucleotide-gated channel 2 (HCN2), HCN4, Na^+-Ca^{2+} exchanger, and Na^+-K^+-ATPase.[2–5] In contrast, although ≈25% of hypothyroid patients have diastolic hypertension,[6] the mechanism for the altered systemic vascular resistance under an abnormal thyroid hormone status is not well understood. To date, a loss of nongenomic vasodilating action of thyroid hormone[7] and atherosclerosis attributable to hypercholesterolemia[8] have been associated with the increased systemic vascular resistance under hypothyroidism.[9] Recently, mRNAs for TR isoforms were identified in aortic and coronary smooth muscle cells, suggesting that a direct genomic action of thyroid hormone may play a significant role in vascular smooth muscle.[10] Although extremely high concentrations of thyroid hormone are known to regulate expression of several genes in vascular smooth muscle cells,[10,11] the physiological and direct target genes of thyroid hormone in vascular smooth muscle cells are not known.[9]

Arterial calcification is a common pathological feature of vascular sclerosis, as well as a variety of metabolic disorders such as diabetes and renal disease. Decades ago, cretinism

Original received October 8, 2004; revision received August 2, 2005; accepted August 3, 2005.

From the Divisions of Cellular and Gene Therapy Products (Y.S., R.N., S.M., T.Y.), Biosignaling (K.F., K.I.), and Pharmacology (S.I., Y.O.), National Institute of Health Sciences (T.N.), Tokyo, Japan; and the Department of Pharmacology and Toxicology (R.N., M.S.), Toho University, Faculty of Pharmaceutical Sciences, Chiba, Japan.

Correspondence to Yoji Sato, PhD, Division of Cellular and Gene Therapy Products, National Institute of Health Sciences, 1-18-1 Kami-yoga, Setagaya, Tokyo 158-8501, Japan. E-mail yoji@nihs.go.jp

Circulation Research **is available at http://circres.ahajournals.org** **DOI: 10.1161/01.RES.0000181431.04290.bd**

was found to be associated with arterial calcification, especially when patients did not receive sufficient thyroid hormone replacement therapy.[12] However, the mechanism for the calcification in cretins has been to date unclear. A subset of vascular smooth muscle cells, named "calcifying vascular cells," was demonstrated recently to undergo osteogenic and chondrogenic differentiation in culture, indicating that some vascular smooth muscle cells still have the potential for multiple lineages.[13] Because thyroid hormone plays a critical role in bone remodeling,[14] we hypothesized that thyroid hormone is also associated with vascular calcification. To test this hypothesis, we investigated the effect of thyroid hormone on vascular smooth muscle calcification and expression profiles of calcification-associated genes in vitro and in vivo, and identified matrix Gla protein (MGP) gene as a target of thyroid hormone in vascular smooth muscle cells.

Materials and Methods

Cell Culture

α-Actin–positive rat aortic smooth muscle cells (RAOSMCs) were obtained from Cell Applications, Inc. and were cultured on 6-well cell culture plates at 37°C in a humidified atmosphere of 95% air/5% CO_2 in growth medium (GM; Dulbecco's Minimal Essential Medium [DMEM] supplemented with 10% FCS, 100 U/mL penicillin, and 100 μg/mL streptomycin). Cells up to passage 5 were used for the experiments. The culture media were changed every 48 hours. Thyroid hormone–depleted serum was prepared as described previously.[15] To evaluate effects of thyroid hormone on gene expression profiles of the synthetic phenotype of RAOSMCs, the cells at 50% of confluence were cultured in thyroid hormone–depleted medium (TDM; DMEM containing 10% thyroid hormone-depleted serum, 100 U/mL penicillin, and 100 μg/mL streptomycin) for 2 days and stimulated with 3′,3,5-triiodo-L-thyronine (T_3) for another 2 days. The contractile form of RAOSMCs was obtained by culturing confluent cells in serum-free differentiation medium (DM; DMEM supplemented with 1× ITS-X (Invitrogen), 5 mmol/L taurine, 100 U/mL penicillin, and 100 μg/mL streptomycin) for 10 days, followed by T_3 treatment for 2 days. The transition of the cell phenotype in DM was confirmed by immunoblotting for nonmuscle myosin heavy chain (SMemb) and smooth muscle myosin heavy chain-2 (SM2). To examine effects of thyroid hormone on calcium accumulation, confluent RAOSMCs were cultured as described previously[16] in TDM with or without 100 ng/mL recombinant human bone morphogenic protein-2 (rBMP2; R & D Systems) in a cell culture dish with or without collagen type IV (Col4) coating (BD Biosciences). Supplementation with β-glycerophosphate, which facilitates smooth muscle cell calcification,[17] was omitted because of a decrease in the signal-to-background ratio. Cells were subsequently stimulated with T_3 for 5 days. The concentrations of free T_3 (fT_3) and free L-thyroxine (T_4) in the serum-containing medium were determined using chemiluminescent enzyme immunoassay at a clinical diagnostic laboratory. The detection limits for fT_3 and fT_4 were 1.1 pmol/L and 1.7 pmol/L, respectively. Human coronary artery smooth muscle cells (HCASMCs; Cell Applications, Inc.) were maintained and transformed into the contractile phenotype before treatment with T_3 by culturing for 7 days in serum-free HCASMC DM (311D-500; Cell Applications, Inc) according to manufacturer instructions.

Animals

Male Sprague-Dawley rats (Japan SLC; Shizuoka, Japan) were maintained on rodent chow (Certified diet MF; Oriental Yeast, Co) and given water ad libitum. For generation of hypothyroid animals, methimazole (MMI; 400 mg/L) was added to the drinking water for 4 weeks. Hyperthyroid rats were generated by daily injection of T_3 (0.2 mg/kg body weight IP) for 10 days. Plasma concentrations of fT_3 and fT_4 were measured, as described above. After the treatment with MMI or T_3, the thoracic aorta was isolated. Animals were 12 weeks old when killed. Aortic smooth muscle tissue for measurements of calcium accumulation and gene expression was cleared of fat, connective tissue, and an endothelium and stored at −80°C until use. For pathological examination, the aortic tissue was fixed in 10% formaldehyde. Transverse aortic sections were taken from the fixed tissue and stained with hematoxylin and eosin. All animals were treated in accordance with laboratory animal care guidelines of National Institute of Health Sciences at Tokyo.

Calcium Accumulation

Calcium content in RAOSMCs and rat aortic smooth muscle tissues were determined as described previously[16] using o-cresolphthalein complexone method. Protein concentration was determined using Bio-Rad protein assay reagent and BSA as a standard.

Real-Time Quantitative RT-PCR

Total RNA was isolated from smooth muscle cells and tissues using Sepasol reagent (Nakalai Tesque) containing 0.1 mg/mL glycogen (Roche Diagnostics) and was treated with DNaseI (Promega) according to the manufacturer protocols. To quantitate specific mRNA levels, the real-time progress of target sequence-specific amplification was monitored during RT-PCR using TaqMan chemistry and PRISM7000 Sequence Detection System (Applied Biosystems). An 18S ribosomal RNA was used as an internal control for each RNA level. Sequences of the primers and the TaqMan probes are listed in supplemental Table I (available online at http://circres.ahajournals.org).

Western Blot Analysis

RAOSMCs and aortic smooth muscle tissues were homogenized in lysis buffer as described previously.[18] After measuring protein concentrations, proteins were separated by SDS-PAGE and blotted onto polyvinylidene fluoride membranes, which were incubated with anti-SMemb or anti-SM2 monoclonal antibodies (Yamasa) or an anti-MGP polyclonal antibody (TransGenic) for 1 hour at room temperature. Subsequently, membranes were incubated with the secondary antibody conjugated with horseradish peroxidase for 1 hour. Signals were visualized and quantified using ECL Plus system (Amersham Biosciences) and LAS-3000 Imaging System (FUJIFILM), respectively.

Promoter Activity Assay

Fragments between −1752 and −1 of 5′ flanking sequence of the MGP gene exon 1 and between −1895 and −1 of 5′ flanking sequence of the stanniocalcin-1 (STC1) gene exon 1 were amplified using rat tail genomic DNA as a template. The primers for PCR amplifications were designed as based on the nucleotide sequences (MGP forward: CAAGGGTACCGGTTTGAGAGACCACGAGAC; MGP reverse: CTTGAAGCTTCCTGTGAGTCTGCCTCTGTG; STC1 forward: CAAGCTCGAGCCCCTGATATTTCAGCATGG; STC1 reverse: CTTGAAGCTTAGGTGAGGATTTGAGGAGG). The amplicons were subcloned into the firefly luciferase expression vector pGL3-Basic (Promega). RAOSMCs in the contractile state, grown on a 24-well plate, were transiently cotransfected with 225 ng/well of each promoter luciferase plasmid and 75 ng/well of phRL-TK control plasmid (Promega) using FuGene6 (Roche). Three hours after transfection, cells were incubated with or without T_3. The luciferase activity was defined as a ratio of the firefly luciferase signal to the renilla luciferase signal, which was measured with Dual-Luciferase Reagent (Promega). The transfection efficiency of the plasmids was estimated to be 1% to 10% of the total RAOSMCs, as assessed by transfection experiments with an enhanced green fluorescent protein expression vector pEGFP-N1 (BD Biosciences Clontech; data not shown).

RNA Interference Against TRα

RAOSMCs in the synthetic form were transiently transfected with StealthRNAi (Invitrogen) specific for TRα gene (sense: CCAGAAGAACCUCCAUCCCACCUAU; antisense: AUAGGUGGGAUG-

Free Thyroid Hormone Concentrations in Rat Plasma and Serum-Containing Cell Culture Medium

Plasma/Medium	fT_3 (pmol/L)	fT_4 (pmol/L)	Calculated Range of Thyroid Hormone Activity (pmol fT_3/L)
Plasma from a euthyroid rat	4.2±0.6	27±2	6.9–31
Plasma from a hypothyroid rat (MMI treatment for 1 month)	<1.1	<1.8	<1.3–2.9
GM (DMEM, 10% FCS, P/S)	3.7±0.2	15±0.0	5.2–19
TDM (DMEM, 10% thyroid hormone–depleted FCS, P/S)	<1.1	2.7±0.2	<1.4–3.8
TDM (DMEM, 10% thyroid hormone–depleted FCS, P/S) + 1 nmol/L T_3	15±1*	3.4±0.1*	15–18

The range of thyroid hormone activity was calculated assuming that X% (X=0–100) of T_4 is processed to T_3 at the site of action in vivo and that the affinity of T_4 for TRs is one tenth that of T_3.

P/S indicates penicillin and streptomycin.

Values are means±SD; *P<0.05 vs TDM without T_3 supplementation (Student t test).

GAGGUUCUUCUGG) or StealthRNAi negative control medium GC (Invitrogen) using Lipofectamine 2000 (Invitrogen), according to manufacturer instructions and incubated in TDM for 2 days. Cells were then treated with or without T_3 (15 pmol/L fT_3) for another 2 days. Total RNA was isolated from cells before and after T_3 treatment for mRNA determinations.

Statistics

Data were expressed as means±SEM unless otherwise indicated. Data were analyzed for statistical significance by Student t test or ANOVA with Student-Newman–Keuls test as a post hoc test. Significance was imparted at the P<0.05 level.

Results

Free Thyroid Hormone Concentrations

As shown in the Table, plasma concentrations of fT_3 and fT_4 in euthyroid rats were 4.2±0.6 pmol/L and 27±2 pmol/L (mean±SD), respectively. The MMI treatment decreased fT_3 and fT_4 to <1.1 pmol/L and to <1.8 pmol/L, respectively, indicating that the animals were hypothyroid. The fT_3 and fT_4 levels in GM containing 10% FCS were 3.7±0.2 pmol/L and 15±0.0 pmol/L (mean±SD), respectively, and happened to be similar to those in plasma from euthyroid rats. The free concentrations of thyroid hormones in TDM (<1.1 pmol/L fT_3; 2.7 pmol/L fT_4) were low enough to keep TRs inactivated because the K_d values of T_3 for TRs are known to be ≈10 to 100 pmol/L[19] and because T_4 has ≈10-fold lower affinity for TRs than that of T_3. In vascular smooth muscle cells, T_4 is known to be converted to T_3 by type II iodothyronine deiodinase,[10] although the conversion rate in vivo is not clear. Assuming that X% (X=0 to 100) of T_4 is processed to T_3 at the site of action in vivo and that the affinity of T_4 for TRs is one tenth of that of T_3, the total activity of thyroid hormones in euthyroid rat plasma should be equivalent to that of 6.9 to 31 pmol/L [4.2+27×X/100+27×(1−X/100)/10] of fT_3 alone. The supplementation of T_3 to TDM at 1 nmol/L of total concentration resulted in an increase in fT_3 to 15±1 pmol/L (mean±SD), with a slight increase in fT_4, therefore, it was regarded within a euthyroid range.

T_3-Induced Gene Expression and Calcification in Cultured RAOSMCs

Vascular smooth muscle cells show a high degree of plasticity and are able to interchange between a differentiated, contractile phenotype and a proliferating, synthetic phenotype. Therefore, we first examined the effects of T_3 on expression profiles of calcification-associated genes in both phenotypes. RAOSMCs in GM predominantly expressed a marker of synthetic phenotype: SMemb. The replacement of the medium with DM reduced the protein level of SMemb to 28% and increased SM2 expression by 11.6-fold (online Figure I), indicating the transition of the phenotype. In the synthetic phenotype, T_3 (1 nmol/L total T_3=15 pmol/L fT_3) led to upregulation of mRNAs for MGP and STC1×3.3-fold and 1.3-fold, respectively (Figure 1A), whereas osteopontin

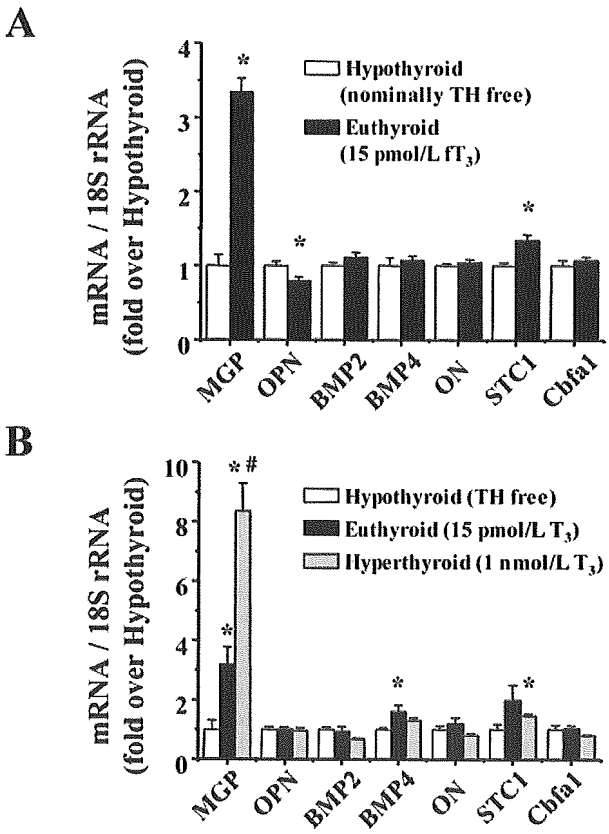

Figure 1. T_3 regulated expression of calcification-associated genes in cultured RAOSMCs in synthetic and contractile forms. A, Effect of T_3 on mRNA expression of calcification-associated genes in the synthetic form of RAOSMCs cultured in TDM. Cells were treated with 15 pmol/L fT_3 for 2 days. B, Effect of T_3 on mRNA expression of calcification-associated genes in the contractile form of RAOSMCs cultured in the DM. Cells were treated with 15 pmol/L or 1 nmol/L T_3 for 2 days. Values are expressed as means±SEM (n=4) TH indicates thyroid hormone. *P<0.05 vs hypothyroid; #P<0.05 vs euthyroid.

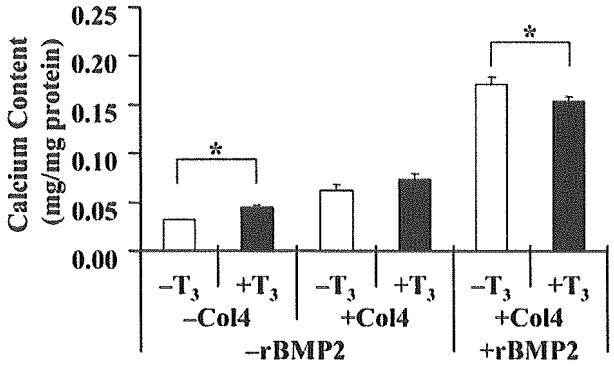

Figure 2. Effects of T_3 on calcium accumulation in cultured RAOSMCs. The confluent cells cultured in TDM were stimulated by 15 pmol/L fT_3. In the absence of rBMP2, T_3 significantly increased calcium content in RAOSMCs cultured in noncoated vessels. Supplementation with rBMP2 increased the basal calcium content in RAOSMCs in Col4-coated vessels and reversed the effect of T_3 on the calcification. Values are expressed as means±SEM (n=6 to 8); *P<0.05.

(OPN) was downregulated by 21%. The mRNA levels of BMP2, bone morphogenic protein-4 (BMP4), osteonectin (ON), and core binding factor α1 (Cbfa1; also known as Runx2 or Osf2) were not significantly altered by the T_3 treatment. Specific signals for osteocalcin and bone sialoprotein mRNA were not detected by several independent primer sets in all experiments of the present study, presumably because of their low abundance in vascular smooth muscle cells. In the contractile phenotype in DM, T_3 (15 pmol/L) induced upregulation of MGP and BMP4×3.2-fold and 1.6-fold, respectively (Figure 1B). A higher concentration of T_3 (1 nmol/L) resulted in a further increase in the MGP mRNA level and a significant upregulation of STC1 mRNA, indicating the dose dependency of the effects. Messenger RNA levels of OPN, BMP2, ON, STC1, and Cbfa1 in the contractile phenotype were not significantly altered by the T_3 treatment. Among the calcification-associated genes, MGP and STC1 genes were commonly upregulated by T_3 in both phenotypes, suggesting that these two genes were relatively essential in RAOSMCs as targets of thyroid hormone.

Because the effect of MGP on calcification and osteogenic differentiation of vascular smooth muscle cells depends on availability of BMP2 and Col4,[20,21] cell calcification was determined in the absence or presence of these factors. In the absence of rBMP2 and Col4 coating, treatment with T_3 (1 nmol/L total T_3=15 pmol/L fT_3) for 5 days resulted in an increase in calcium content by 39% in RAOSMCs (Figure 2). The same treatment tended to have the similar effect on cells in a Col4-coated vessel in the absence of rBMP2. In contrast, T_3 led to a significant decrease in cellular calcium by 10% in the presence of rBMP2 and Col4-coating.

Transcriptional Regulation of MGP and STC1 Genes by T_3

To test a hypothesis that the promoters of MGP and STC1 genes were under regulation of thyroid hormone, RAOSMCs were transiently transfected with luciferase reporters under control of the MGP and STC1 promoters. The 5′ flanking sequences of MGP and STC1 genes have been submitted to

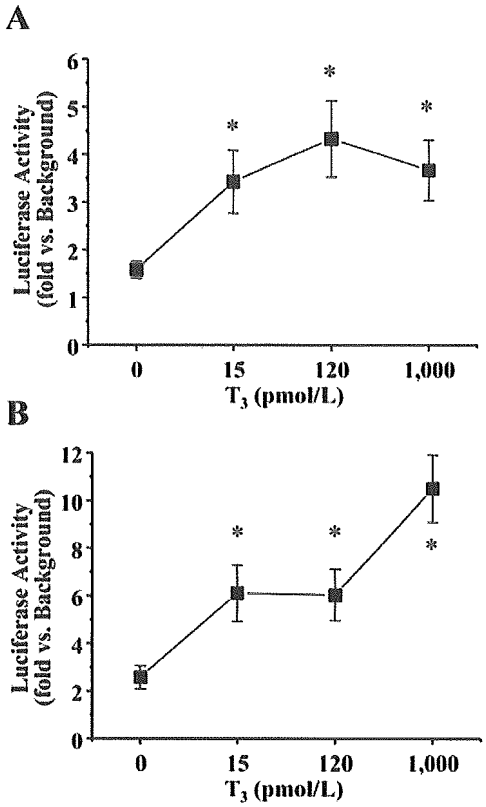

Figure 3. T_3 activated luciferase reporter genes driven by rat MGP (A) and STC1 (B) promoters in the contractile form of RAOSMCs. Cells were transiently cotransfected with a reporter plasmid containing a promoter region of rat MGP or STC1 gene and an internal control plasmid (phRL-tk) and were treated with T_3 for 2 days. The cell extracts were assayed for luciferase activity. Values are normalized to the background (luciferase activity of the cells transfected with promoterless pGL3-Basic vector and phRL-tk) and expressed as means±SEM (n=6); *P<0.05 vs control.

NCBI (accession numbers AY750958 and AY750959, respectively). Transcription Element Search System (TESS)[22] revealed that consensus sequences of the thyroid hormone response element were located in 585 to 600 (*TGTACCCAATGAACC*) and 1009 to 1024 (*TGGAGACAGGAGGACA*) bases upstream of the putative transcription initiation sites of MGP and STC1 genes, respectively. Treatments of the cells with T_3 (15 pmol/L to 1 nmol/L) for 48 hours resulted in significant increases in transcriptional activity compared with vehicle treatment (Figure 3).

Regulation of MGP and STC1 Expression via TRs

Arterial smooth muscle cells express TRα1 and TRα2 nuclear receptor isoforms strongly and TRβ1 and TRβ2 relatively weakly.[10] To evaluate the involvement of TRs in the T_3-induced upregulation of MGP and STC1 mRNAs, RNA interference (RNAi) was performed using StealthRNAi specific for the TRα gene encoding TRα1 and TRα2. The RNAi in RAOSMCs for 2 days significantly attenuated mRNA expression of TRα1 and TRα2 by 66% and 57%, respectively, compared with the controls (Figure 4). The RNAi was also associated with upregulation of MGP mRNA by 32%

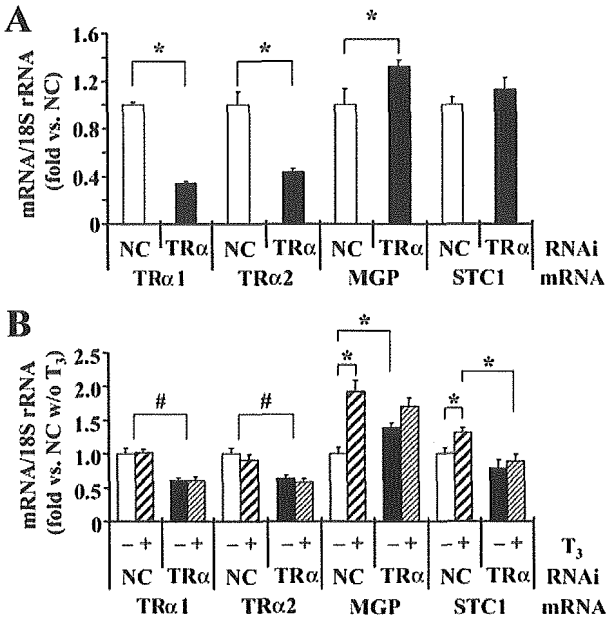

Figure 4. The RNAi against TRα gene in RAOSMCs (synthetic form). A, RNAi against TRα gene for 2 days led to significant decreases in expression of TRα1 and TRα2 to the same extent and a slight increase in the MGP expression. B, The expression of TRα1 and TRα2 remained reduced after the following incubation for 2 more days and was not altered by T_3 (15 pmol/L fT_3). The RNAi was associated with loss of responsiveness of MGP and STC1 mRNA to T_3. Values are expressed as means±SEM (n=4 to 6 [A] and 8 [B]). NC indicates negative control. *P<0.05 (Student t test [A] or Student-Newman–Keuls test [B]); #P<0.05 association with RNAi (two-way ANOVA).

compared with the controls, suggesting that unliganded TRα1 or TRα2, which has no affinity for thyroid hormones, had an inhibitory effect on the expression of MGP. The mRNA level of STC1 was not altered by the RNAi. Incubation with 15 pmol/L fT_3 for the following 2 days facilitated the expression of MGP and STC1 in the control group, whereas no significant effect of T_3 on MGP and STC1 gene expression was detected in the RNAi group. T_3 had no effect on the expression of the TRα isoforms.

Calcium Accumulation in Hypothyroid Rat Aorta

As examined by hematoxylin-eosin staining, the cross-sections of aorta from rats treated with MMI for 4 weeks did not show obvious calcified foci (Figure 5A). However, *o*-cresolphthalein complexone experiments indicated that the 4-week treatment with MMI significantly increased the calcium content in the rat aortic smooth muscle tissues by 33% compared with that of euthyroid animals (Figure 5B). Quantitative RT-PCRs revealed that mRNA levels of MGP, BMP4, ON, and Cbfa1 were downregulated by 68%, 87%, 69%, and 72%, respectively, by the MMI treatment. OPN, BMP2, and STC1 mRNA levels were not significantly altered (Figure 5C). MMI also attenuated protein expression of MGP by 54% (Figure 5D). Calcified foci were not observed even in aortic cross-sections from rats treated with MMI for 12 weeks (online Figure II), suggesting that the calcification was not progressive.

Calcium Content in Hyperthyroid Rat Aorta

Hyperthyroidism elicits pronounced vascular relaxation.[9] However, the effect of hyperthyroidism on vascular calcification has been unclear. Therefore, it is of interest to compare effects of hyperthyroidism on the expression profiles of calcification-associated genes with those of hypothyroidism. In contrast to the aortic smooth muscle from hypothyroid rats, daily injections of T_3 for 10 days led to a decrease in the calcium content in the rat aortic smooth muscle tissues by 11% compared with that of euthyroid animals (Figure 6A). Quantitative RT-PCRs showed that mRNA levels of MGP, OPN, and BMP2 were upregulated by 4.5-fold, 4.9-fold, and 3.4-fold, respectively, by the T_3 treatment, whereas hyperthyroidism resulted in a significant decrease in the level of STC1 mRNA (Figure 6B).

Upregulation of MGP mRNA in Cultured HCASMCs

To demonstrate that thyroid hormone regulates MGP gene expression in vascular smooth muscle cells of a different species, we determined MGP mRNA levels in HCASMCs in the presence and absence of T_3. Treatment with a physiological concentration (15 pmol/L) of T_3 for 2 days led to a significant increase in MGP mRNA by 40% (1.0±0.07 [hypothyroid 0 pmol/L T_3] versus 1.40±0.13 [euthyroid 15 pmol/L T_3] in an arbitrary unit; n=12).

Discussion

In the present study, thyroid hormone led to an upregulation of MGP in arterial smooth muscle cells in vitro regardless of culture condition, phenotype, and animal species of the cells. The transcriptional activity of the MGP gene was increased by T_3, and reduction of TRα gene expression led to a loss of responsiveness of the MGP gene to T_3, suggesting that the effect of T_3 is based on a genomic action via TRα1. Furthermore, in vivo hormone levels were positively and negatively associated with the expression of MGP and calcification in vascular smooth muscle, respectively. Because aortic smooth muscle from hypothyroid rats showed no obvious neointimal formation, the vascular calcification under the hypothyroidism is likely to be similar to that of media sclerosis. In aortic smooth muscle from hypothyroid rats, expression levels of calcification activators BMP4, ON, and Cbfa1 were decreased, whereas hyperthyroidism upregulated another calcification activator BMP2. However, calcium content in aortic smooth muscle was increased in hypothyroidism, and the opposite was observed in hyperthyroidism, suggesting that the expression or function of calcification inhibitors, such as MGP and OPN, are more dominant for the phenotypic outcome in vivo, compared with those of the calcification activators.

MGP is a mineral-binding extracellular matrix protein synthesized by vascular smooth muscle cells and chondrocytes. Luo et al have shown that ablation of MGP gene in mice causes extensive and lethal calcification and cartilaginous metaplasia of the media of all elastic arteries, indicating that MGP has an inhibitory effect on media calcification in vivo.[23] In contrast, in the same study, morphological analysis showed that heterozygous MGP knockout mice, which had a

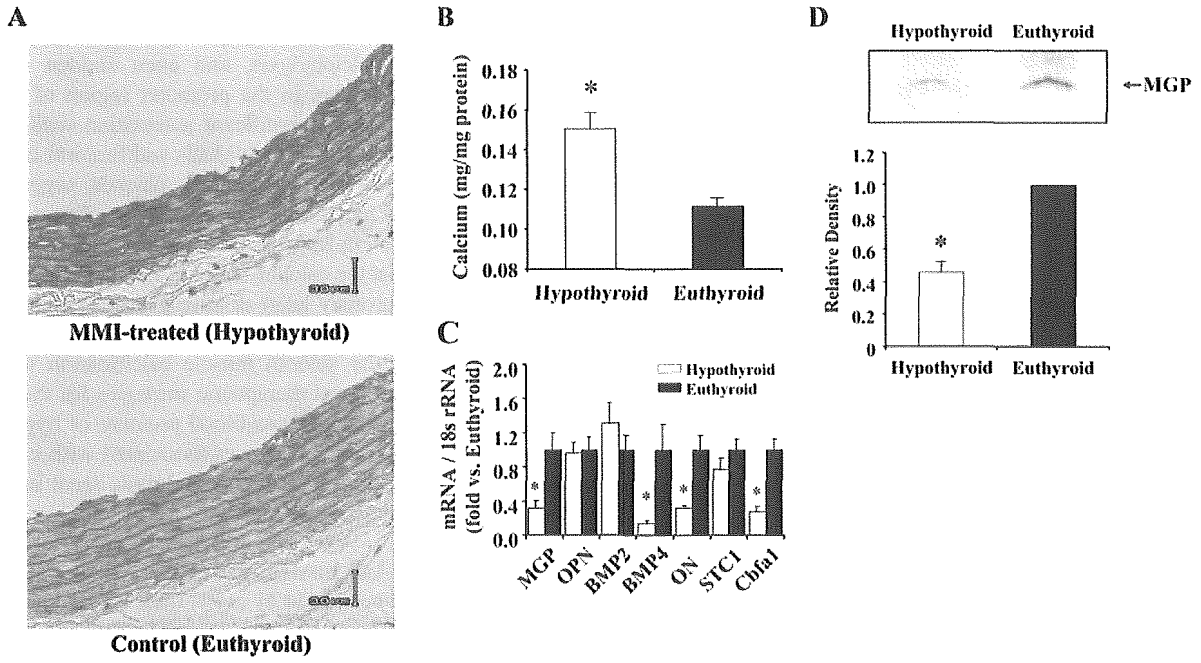

Figure 5. Hypothyroidism led to calcium accumulation in aortic smooth muscle and an altered expression profile of calcification-associated genes. Hypothyroidism was achieved by treatment of the animals with MMI (400 mg/L drinking water) for 4 weeks. A, Hematoxylin-eosin staining of cross-sections of aortae from euthyroid and hypothyroid rats. No obvious calcified foci were observed in either section. Bar=30 μm. B, Effect of the hypothyroidism on calcium deposition in rat aortic smooth muscle. C, Effect of hypothyroidism on mRNA expression of calcification-associated genes in rat aortic smooth muscle. D, Effect of hypothyroidism on MGP protein expression in rat aortic smooth muscle. Values are expressed as means±SEM (n=7 to 8); *P<0.05 vs euthyroid.

similar decrease in an arterial MGP level to that by the MMI treatment in the present study, had no obvious calcified foci in arterial smooth muscle. However, this does not necessarily imply that the heterozygous ablation of MGP gene does not affect calcium content in arteries because biochemical quantification for tissue calcium has not been performed. Thus, it is still possible that there is a dose-response relationship between MGP and media calcification, and that an ≈50% reduction of MGP results in some increase in calcium content, although it may not be morphologically evident.

The extracellular environment around smooth muscle cells is known to determine a functional role of MGP. Namely, calcification of vascular smooth muscle cells in the presence of a relatively high concentration of BMP2 was inhibited by MGP, whereas calcification of vascular smooth muscle cells under a low concentration of BMP2 was stimulated by MGP.[20] Moreover, extracellular matrix proteins, especially Col4, have significant influence on MGP function and vascular calcification.[21] In fact, the effect of T_3 on calcification of RAOSMCs was determined by these environmental factors. Therefore, these results suggest that T_3 regulates smooth muscle cell calcification, at least partly, by promoting MGP expression, although not only vascular cells but also migratory adventitial pericytic myofibroblasts and circulating skeletal progenitors may have some additional contributions to vascular calcification in vivo.[24]

STC1 is a mammalian homolog of stanniocalcin, the fish calcium/phosphate- regulating polypeptide that inhibits calcium flux into cells and stimulates phosphate reabsorption. In the present study, gene transcription of STC1 appeared to be regulated by T_3 via TRα in a dose-dependent manner. However, the highest mRNA expression of STC1 tended to be achieved at a euthyroid status in vitro and in vivo, and hyperthyroidism significantly attenuated the STC1 mRNA expression in vivo. Recently, STC1 was shown to accelerate osteoblast development in an autocrine/paracrine manner in cultured fetal rat calvaria cells.[25] Therefore, the downregulation of STC1 may also contribute to the low calcium content in aortic smooth muscle of hyperthyroid rats, although the mechanism that offsets the increase in the STC1 gene transcription remains to be elucidated.

OPN is known to inhibit or promote vascular smooth muscle calcification in vivo in a phosphorylation-dependent manner.[26] Therefore, the changes in its expression in the synthetic form of RAOSMCs and in smooth muscle tissue of hyperthyroid rats may be also associated with the effect of thyroid hormone on calcium accumulation. However, as shown in the in vitro and MMI experiments, a physiological concentration of thyroid hormone is unlikely to target OPN gene directly, at least in the contractile form of aortic smooth muscle cells.

BMP2 was upregulated by hyperthyroidism in vivo, whereas BMP4 was downregulated by MMI-induced hypothyroidism. BMP2 is know to antagonize the effect of MGP,[20] and BMP4 has been suggested to play a significant role as a cytokine, a growth factor or a media-calcification promoter in vascular lesions of calciphylaxis.[27] The mRNA levels of ON and Cbfa1 were also decreased in hypothyroid rat aortic smooth muscle. With the exception of BMP4, these changes in vivo did not follow on from the in vitro experiments,

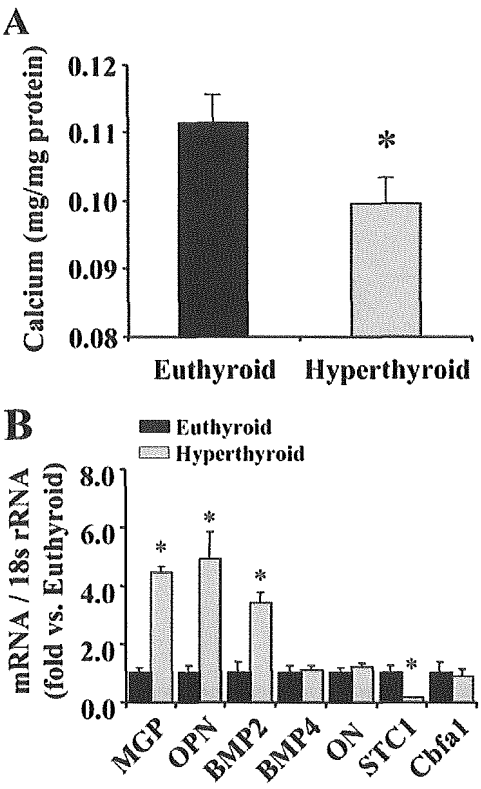

Figure 6. Hyperthyroidism decreased tissue calcium content in aortic smooth muscle and altered the expression profile of calcification-associated genes. Hyperthyroidism was achieved by daily injection of T_3 (0.2 mg/kg body weight IP) for 10 days. A, Effect of the hyperthyroidism on calcium deposition in rat aortic smooth muscle. C, Effect of hyperthyroidism on mRNA expression of calcification-associated genes in rat aortic smooth muscle. Values are expressed as means±SEM (n=7 to 8); *$P<0.05$ vs euthyroid.

suggesting that the alterations were not attributable to a direct effect of thyroid hormone on vascular smooth muscle cells. Because physiological concentrations of thyroid hormones upregulated BMP4 in the contractile form of RAOSMCs and in vivo (hypothyroid versus euthyroid), BMP4 may be another direct target of thyroid hormone in aortic smooth muscle cells. However, the expected influences of the changes in all the calcification activators above were apparently masked, aforementioned, indicating their minor roles in vascular calcification, compared with those of calcification inhibitors.

In summary, our findings, for the first time, demonstrate that a physiological concentration of thyroid hormone has significant genomic effects on vascular smooth muscle cells in vitro and in vivo, which are associated with vascular calcification. Most notably, a decrease in thyroid hormone and the concomitant increase in vascular calcification in vivo are marked by a decrease in the level of MGP expression, suggesting that a physiological concentration of thyroid hormone has a direct protective role against vascular smooth muscle calcification in vivo. Although vascular calcification has been thought to be benign, arterial calcification should alter vascular compliance. Thus, it is possible that the increased vascular stiffness underlies the high systemic vascular resistance observed in hypothyroidism. Vascular calcification can lead to some other serious problems, including vascular stenosis, calciphylaxis, and even sudden death. Recently, a polymorphism in the promoter region of MGP gene was found to have a significant association with myocardial infarction in low-risk individuals and femoral calcification in the presence of atherosclerotic plaques, suggesting involvement of this mutation in coronary artery disease.[28] In addition, a recent meta-analysis of coronary artery calcium scores suggested that the calcium score is an independent risk factor to predict coronary heart disease events.[29] Therefore, further studies on the protective role of thyroid hormone and MGP against vascular smooth muscle calcification should provide insights into novel therapeutic strategies for the high systemic vascular resistance and blood pressure of hypothyroid patients, as well as for diseases associated with cardiovascular calcification such as diabetes, chronic renal insufficiency, and hypercholesterolemia.

Acknowledgments

This work was supported in part by grants from Japan Ministry of Health, Labor, and Welfare (H17-SAISEI-021), Japan Ministry of Education, Culture, Sports, Science, and Technology (13770052 and 15790141), the Japan Health Sciences Foundation (KH23106), and the Pharmaceuticals and Medical Devices Agency (MF-16).We thank Dr Youichi Shinozaki, Hidetoshi Tozaki, and Hiromi Yoshida for excellent technical assistance, and Dr Helen Kiriazis (Baker Heart Research Institute, Melbourne) for critical reading of this manuscript.

References

1. Carr AN, Kranias EG. Thyroid hormone regulation of calcium cycling proteins. *Thyroid*. 2002;12:453–457.
2. Abe A, Yamamoto T, Isome M, Ma M, Yaoita E, Kawasaki K, Kihara I, Aizawa Y. Thyroid hormone regulates expression of shaker-related potassium channel mRNA in rat heart. *Biochem Biophys Res Commun*. 1998;245:226–230.
3. Gloss B, Trost S, Bluhm W, Swanson E, Clark R, Winkfein R, Janzen K, Giles W, Chassande O, Samarut J, Dillmann W. Cardiac ion channel expression and contractile function in mice with deletion of thyroid hormone receptor alpha or beta. *Endocrinology*. 2001;142:544–550.
4. Boerth SR, Artman M. Thyroid hormone regulates Na^+-Ca^{2+} exchanger expression during postnatal maturation and in adult rabbit ventricular myocardium. *Cardiovasc Res*. 1996;31:E145–E152.
5. Orlowski J, Lingrel JB. Thyroid and glucocorticoid hormones regulate the expression of multiple Na,K-ATPase genes in cultured neonatal rat cardiac myocytes. *J Biol Chem*. 1990;265:3462–3470.
6. Klein I, Ojamaa K. Thyroid hormone and the cardiovascular system. *N Engl J Med*. 2001;344:501–509.
7. Ojamaa K, Klemperer JD, Klein I. Acute effects of thyroid hormone on vascular smooth muscle. *Thyroid*. 1996;6:505–512.
8. Hak AE, Pols HAP, Visser TJ, Drexhage HA, Hofman A, Witteman JC. Subclinical hypothyroidism is an independent risk factor for atherosclerosis and myocardial infarction in elderly women: the Rotterdam Study. *Ann Intern Med*. 2000;132:270–278.
9. Klein I, Ojamaa K. Thyroid hormone: targeting the vascular smooth muscle cell. *Circ Res*. 2001;88:260–261.
10. Mizuma H, Murakami M, Mori M. Thyroid hormone activation in human vascular smooth muscle cells: expression of type II iodothyronine deiodinase. *Circ Res*. 2001;88:313–318.
11. Fukuyama K, Ichiki T, Takeda K, Tokunou T, Iino N, Masuda S, Ishibashi M, Egashira K, Shimokawa H, Hirano K, Kanaide H, Takeshita A. Downregulation of vascular angiotensin II type 1 receptor by thyroid hormone. *Hypertension*. 2003;41:598–603.
12. Komar NN, Gabrielsen TO. Arterial calcification in adult cretins. *Am J Roentgenol Radium Ther Nucl Med*. 1967;101:202–203.
13. Tintut Y, Alfonso Z, Saini T, Radcliff K, Watson K, Bostrom K, Demer LL. Multilineage potential of cells from the artery wall. *Circulation*. 2003;108:2505–2510.

14. Bassett JH, Williams GR. The molecular actions of thyroid hormone in bone. *Trends Endocrinol Metab.* 2003;14:356–364.
15. Samuels HH, Stanley F, Casanova J. Depletion of L-3,5,3′-triiodothyronine and L-thyroxine in euthyroid calf serum for use in cell culture studies of the action of thyroid hormone. *Endocrinology.* 1979; 105:80–85.
16. Jono S, Nishizawa Y, Shioi A, Morii H. Parathyroid hormone-related peptide as a local regulator of vascular calcification. Its inhibitory action on in vitro calcification by bovine vascular smooth muscle cells. *Arterioscler Thromb Vasc Biol.* 1997;17:1135–1142.
17. Shioi A, Nishizawa Y, Jono S, Koyama H, Hosoi M, Morii H. Beta-glycerophosphate accelerates calcification in cultured bovine vascular smooth muscle cells. *Arterioscler Thromb Vasc Biol.* 1995;15: 2003–2009.
18. Sato Y, Ferguson DG, Sako H, Dorn GW II, Kadambi VJ, Yatani A, Hoit BD, Walsh RA, Kranias EG. Cardiac-specific overexpression of mouse cardiac calsequestrin is associated with depressed cardiovascular function and hypertrophy in transgenic mice. *J Biol Chem.* 1998;273:28470–28477.
19. Lazar MA, Chin WW. Nuclear thyroid hormone receptors. *J Clin Invest.* 1990;86:1777–1782.
20. Zebboudj AF, Shin V, Bostrom K. Matrix GLA protein and BMP-2 regulate osteoinduction in calcifying vascular cells. *J Cell Biochem.* 2003;90:756–765.
21. Shin V, Zebboudj AF, Bostrom K. Endothelial cells modulate osteogenesis in calcifying vascular cells. *J Vasc Res.* 2004;41:193–201.
22. Schug J, Overton GC. TESS: Transcription Element Search Software on the WWW. In: *Technical Report CBIL-TR-1997–1001-v0.0,* Computational Biology and Informatics Laboratory, School of Medicine, University of Pennsylvania, 1997:1–10.
23. Luo G, Ducy P, McKee MD, Pinero GJ, Loyer E, Behringer RR, Karsenty G. Spontaneous calcification of arteries and cartilage in mice lacking matrix GLA protein. *Nature.* 1997;386:78–81.
24. Vattikuti R, Towler DA. Osteogenic regulation of vascular calcification: an early perspective. *Am J Physiol Endocrinol Metab.* 2004;286: E686–E696.
25. Yoshiko Y, Maeda N, Aubin JE. Stanniocalcin 1 stimulates osteoblast differentiation in rat calvaria cell cultures. *Endocrinology.* 2003;144: 4134–4143.
26. Jono S, Peinado C, Giachelli CM. Phosphorylation of osteopontin is required for inhibition of vascular smooth muscle cell calcification. *J Biol Chem.* 2000;275:20197–20203.
27. Griethe W, Schmitt R, Jurgensen JS, Bachmann S, Eckardt KU, Schindler R. Bone morphogenic protein-4 expression in vascular lesions of calciphylaxis. *J Nephrol.* 2003;16:728–732.
28. Herrmann SM, Whatling C, Brand E, Nicaud V, Gariepy J, Simon A, Evans A, Ruidavets JB, Arveiler D, Luc G, Tiret L, Henney A, Cambien F. Polymorphisms of the human matrix gla protein (MGP) gene, vascular calcification, and myocardial infarction. *Arterioscler Thromb Vasc Biol.* 2000;20:2386–2393.
29. Pletcher MJ, Tice JA, Pignone M, Browner WS. Using the coronary artery calcium score to predict coronary heart disease events. A systematic review and meta-analysis. *Arch Intern Med.* 2004;164: 1285–1292.

Riccardin C: A natural product that functions as a liver X receptor (LXR)α agonist and an LXRβ antagonist

Norimasa Tamehiro[a], Yoji Sato[a], Takuo Suzuki[a], Toshihiro Hashimoto[b], Yoshinori Asakawa[b], Shinji Yokoyama[c], Tohru Kawanishi[a], Yasuo Ohno[a], Kazuhide Inoue[a], Taku Nagao[a], Tomoko Nishimaki-Mogami[a,*]

[a] *National Institute of Health Sciences, Kamiyoga 1-18-1, Setagaya-ku, Tokyo 158-8501, Japan*
[b] *Faculty of Pharmaceutical Sciences, Tokushima Bunri University, Tokushima, Japan*
[c] *Biochemistry, Cell Biology and Metabolism, Nagoya City University Graduate School of Medical Sciences, Nagoya, Japan*

Received 11 July 2005; revised 25 August 2005; accepted 25 August 2005

Available online 12 September 2005

Edited by Ned Mantei

Abstract Liver X receptors (LXRs) α and β share considerable sequence homology and several functions, respond to the same endogenous and synthetic ligands, and play critical roles in maintaining lipid homeostasis. In this study, liverwort-derived riccardin C (RC) and F (RF) were identified as an LXRα agonist/LXRβ antagonist and an LXRα antagonist, respectively. RC and RF bound to LXRs, but had different abilities to recruit a coactivator and thereby induce transactivation. Despite its unique subtype-selective activity, RC enhanced ABCA1 and ABCG1 expression and cellular cholesterol efflux in THP-1 cells. RC may provide a novel tool for identifying subtype-function and drug development.

Keywords: Liver X receptor; ATP-binding cassette transporter A1; ATP-binding cassette transporter G1; HDL; Cholesterol

1. Introduction

The liver X receptors α and β (LXRα and LXRβ) are nuclear receptors that form obligate heterodimers with retinoid X receptor (RXR) [1]. LXRs are activated by several oxysterols or intermediates in the cholesterol synthetic pathway [2,3] and serve as key regulators of cholesterol homeostasis by coordinately regulating several genes involved in the efflux, transport, and excretion of cholesterol. These genes include ATP-binding cassette transporter (ABC) A1, ABCG1, and apolipoprotein E – which mediate cellular cholesterol efflux; cholesterol 7α-hydroxylase – the rate liming enzyme for the conversion of cholesterol to bile acids in the liver; and ABCG5/ABCG8–transporters involved in cholesterol /sterol excretion from the liver and intestine [1]. LXR activation also upregulates genes involved in fatty acid and triglyceride synthesis by inducing sterol regulatory element-binding protein-1c (SREBP-1c) – the master regulator of genes involved in lipogenesis [4–6] – and fatty acid synthase expression [7].

LXRα and LXRβ share a high degree of amino acid similarity (78%), have similar binding affinities to physiological oxysterol ligands [2,3], and have several common functions, including the upregulation of ABCA1 and ABCG1 expression [8,9]. However, these receptors have different tissue distributions: while LXRβ is ubiquitously expressed, the expression of LXRα is limited to the liver, kidney, intestine, adipose tissue, and macrophages [10]. In the liver, LXRα serves as an important regulator of cholesterol catabolism. Mice lacking LXRα has no resistance to dietary cholesterol and fail to upregulate hepatic cholesterol 7α-hydroxylase [11,12], whereas LXRβ null mice maintain their resistance. The role of LXR subtypes in triglyceride metabolism is uncertain. One study has shown a reduction in the liver triglyceride level of LXRβ null mice on standard diet [13], whereas a reduction in the expression of lipogenic genes was observed in LXRα null mice fed cholesterol [11,12]. Thus, selective agonists for each LXR subtype may be necessary to elucidate their precise functions.

Riccardin C (RC) and F (RF) are non-sterol natural products isolated from liverworts [14,15] (Fig. 1A). In the present study, we discovered that RC functions as an LXRα-selective agonist/LXRβ antagonist but effectively enhances cholesterol efflux from THP-1 cells.

2. Materials and methods

2.1. Riccardins C and F

RC and RF were purified from a methanol extract of the liverwort *Blasia pusilla* as described previously [14,15].

2.2. Transient transfections and reporter gene assay

CV-1 cells maintained in DMEM containing 10% FCS were co-transfected with 248 ng of LXR response element (LXRE)-driven luciferase vector (pLXRE$_X$4-tk-Luc), 248 ng of pSV-β-galactosidase control vector (Promega), and 1.25 ng each of pcDNA3.1-LXRα or LXRβ and pcDNA3.1-RXRα with Polyfect (Qiagen) in 24-well plates according to a previously described method [16]. Three hours after transfection, the cells were treated with test compounds in DMEM containing 10% delipidated FBS, 20 μM compactin, and 10 μM mevalonic acid for 24 h. The cells were then lysed and the reporter gene activity was determined. Luciferase activity was normalized to that of β-galactosidase for each well.

*Corresponding author.
E-mail address: mogami@nihs.go.jp (T. Nishimaki-Mogami).

Abbreviations: LXR, liver X receptor; RXR, retinoid X receptor; ABC, ATP-binding cassette transporter; SREBP-1c, sterol regulatory element-binding protein-1c; LXRE, LXR response element; 22(*R*)HC, 22(*R*)-hydroxycholesterol; TO-1317, TO-901317

0014-5793/$30.00 © 2005 Published by Elsevier B.V. on behalf of the Federation of European Biochemical Societies.
doi:10.1016/j.febslet.2005.08.054

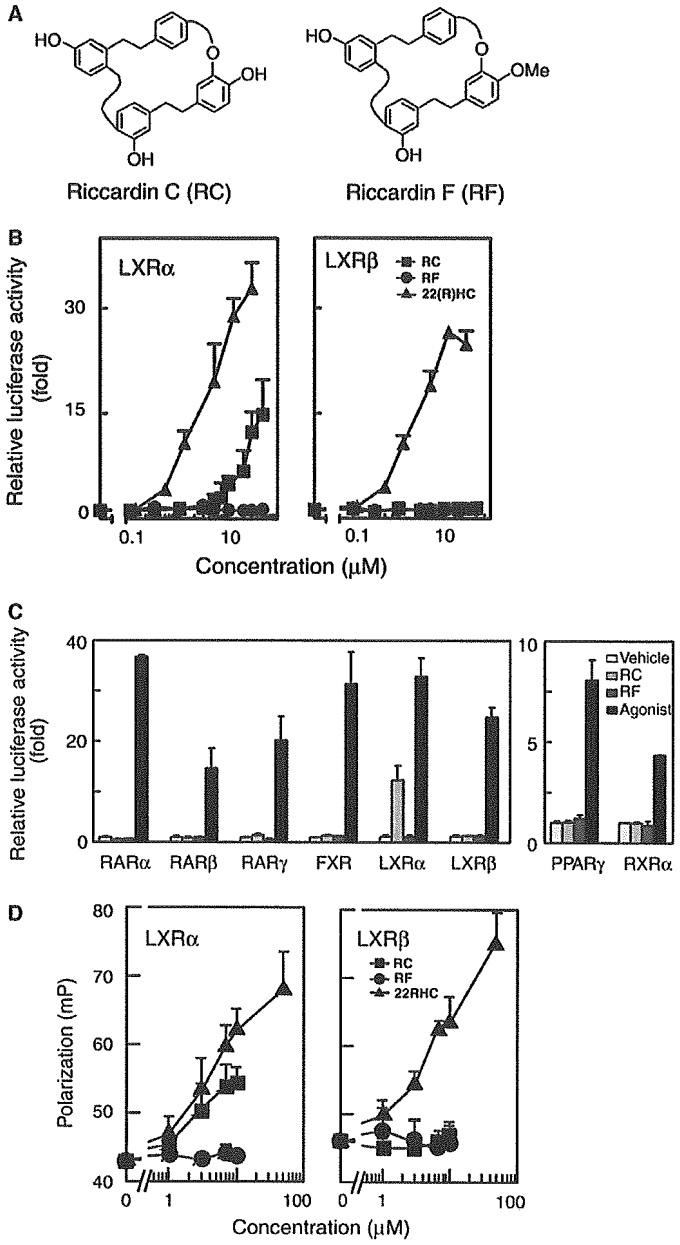

Fig. 1. RC activates LXRα but not LXRβ. (A) Chemical structures of RC and RF. (B) CV-1 cells were transfected with a reporter plasmid (pLXRE$_X$4-tk-*Luc*) and expression plasmids for LXRα (or LXRβ) and RXRα, together with a β-galactosidase as an internal control, and were treated for 24 h with various concentrations of RC, RF, or 22(*R*)HC. Luciferase activity in the cell extracts was normalized using β-galactosidase and expressed as the fold induction relative to vehicle-treated cells. The values are the means ± S.D. of six experiments. (C) Effects of RC and RF on transcriptional activities of heterodimers between RXRα and RARα, RARβ, RARγ, FXR, LXRα, or LXRβ, and RXRα homodimers. CV-1 cells were transfected with expression plasmids for receptors and a β-galactosidase together with a reporter plasmid (pDR5$_X$3-cmv-*Luc* for RARs, pFXRE$_X$4-tk-*Luc*, or pDR1$_X$4-cmv-*Luc* for RXRα), or a PPARγ-Gal4-expression plasmid with a pGal4-UAS-*Luc*. The cells were exposed to RC (30 μM), RF (30 μM), or receptor-specific agonists (3 μM all-trans retinoic acid for RARs and RXRα, 30 μM chenodeoxycholic acid for FXR, 20 μM 22(*R*)HC for LXRs, 30 μM ciglitazone for PPARγ) for 24 h before assaying luciferase activity. The values are the means ± S.D. ($n = 3$). (D) Purified GST-LXRα or GST-LXRβ ligand binding domain was incubated with a fluorescence-tagged SRC-1 peptide and various concentrations of RC, RF, or 22(*R*)HC. The association of ligand-induced SRC-1 peptide with the receptor was monitored by evaluating the increases in millipolarization fluorescence units (mP). The values are the means ± S.D. of six experiments.

2.3. Coactivator association assay using fluorescence polarization

A coactivator association assay using fluorescence polarization was performed according to a previously described method [16]. A TAMRA-labeled peptide (0.1 μM with the amino acid sequence ILRKLLQE) was incubated with purified 1.5 μM GST-fused human LXRα ligand binding domain or LXRβ ligand binding domain in 100 μl of buffer (10 mM HEPES, 150 mM NaCl, 2 mM $MgCl_2$, and 5 mM DTT at pH 7.9) in 96-well black polypropylene plates. After 1-h incubation at room temperature, ligand-dependent recruitment of the coactivator-peptide was measured as the increase in fluorescence polarization using a Fluorescence Plate Reader Fusionα (Perkin–Elmer Life Science).

2.4. Real-time quantitative reverse transcription-PCR

Gene-specific mRNA quantitation was performed by real-time RT-PCR on an ABI Prism 7700 sequence detection system (Applied Biosystems). THP-1 cells maintained in RPMI 1640 medium (Sigma) containing 10% FCS were subcultured in 6-well plates and treated with test compounds in RPMI 1640 containing 0.2% bovine serum albumin. Total RNA extracted from cells using an RNeasy Kit (Qiagen) was treated with DNase according to the manufacturer's instructions. The relative mRNA expression levels were determined using the TaqMan one-step RT-PCR Master Mix (PE Applied Biosystems). The primer/probe sequences for human ABCA1, ABCG1, and SREBP-1c have been previously reported [17].

2.5. Measurement of lipid efflux to apolipoprotein A-I

The lipid efflux measurements were performed according to a previously described method [18]. Briefly, THP-1 cells were treated with the test compounds and 0 or 10 μg/ml of human apoA-I, isolated from the plasma HDL fraction, in RPMI 1640 containing 0.2% bovine serum albumin for 24 h. The lipids were extracted and the cholesterol level was determined using enzymatic methods.

2.6. Statistical analysis

Data were analyzed by ANOVA followed by the Student–Newman–Keuls method.

3. Results

3.1. Identification of RC as an LXRα Agonist

To discover novel LXR agonists, we screened a variety of natural products using a transient transfection assay. CV-1 cells were cotransfected with an LXRE-driven luciferase reporter plasmid and expression plasmids for human LXRα (or LXRβ) and RXRα. RC and RF (Fig. 1A) are novel macrocyclic bis(bibenzyl) dimers isolated from the liverwort [14,15]. Upon cotransfection with LXRα/RXR, RC (30 μM) raised the transactivation of the reporter gene by approximately 15-fold, while a natural LXR agonist, 22(*R*)-hydroxycholesterol (22(*R*)HC), resulted in a 30-fold increase (Fig. 1B). At higher concentrations, RC caused a decrease in β-galactosidase activity. LXRβ/RXRα-dependent transactivation was unaffected by this compound. RF, a 14-methoxyl derivative of RC, activated neither LXRα nor LXRβ. Furthermore, neither RC nor RF activated heterodimers between RXRα and RARα, RARβ, RARγ, FXR, or PPARγ, and RXRα homodimers in cell-based luciferase assays (Fig. 1C).

In an in vitro coactivator-recruitment assay, RC (up to 10 μM) induced a dose-dependent interaction between SRC-1

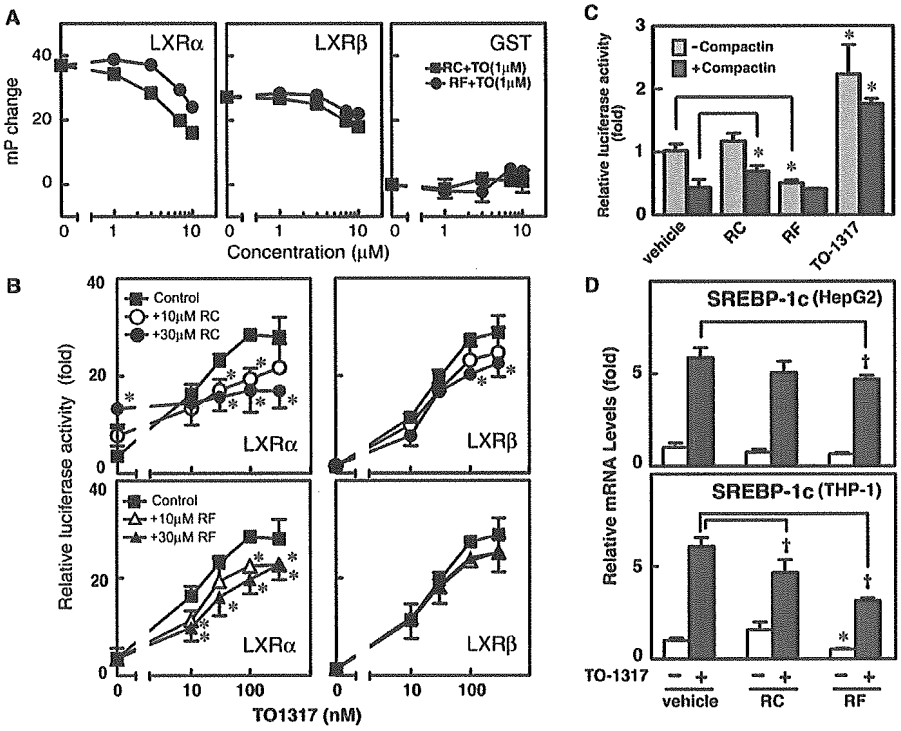

Fig. 2. RC competes with endogenous or synthetic ligands for LXR activation. (A) Fluorescence-tagged SRC-1 peptide was incubated with GST-LXRα, GST-LXRβ, or GST. The changes in fluorescence polarization caused by 1 μM TO-1317 in the presence of the indicated concentrations of RC or RF are shown. A blank value in the absence of ligands was subtracted from the measured values. The values are the means ± S.D. ($n = 3$). (B) CV-1 cells were transfected with pLXRE$_x$4-tk-*Luc* and either LXRα/RXRα or LXRβ/RXRα plasmids, as shown in Fig. 1B, and treated for 24 h with various concentrations of TO-1317 with or without RC or RF (10 or 30 μM). The values are the means ± S.D. of three experiments performed in triplicate. Data were normalized to no ligand control (take as 1) and 100 nM TO-1317 values of a representative experiment. Significantly different from respective controls (*, $P < 0.05$). (C) HepG2 cells were transfected with pLXRE-tk-*Luc* and treated for 24 h with RC (30 μM) or TO-1317 (10 nM) with or without compactin (50 μM) and mevalonic acid (40 μM). The values are the means ± S.D. of three experiments performed in triplicate. Significantly different from respective controls (*, $P < 0.05$). (D) THP-1 cells and HepG2 cells were treated for 24 h with the vehicle (DMSO) alone, RC or RF (30 μM) in the presence or absence of 100 nM TO-1317. SREBP-1c mRNA level was measured by TaqMan quantitative real-time PCR. Data were normalized to 18S rRNA levels and are expressed as the fold induction relative to that in the vehicle-treated cells. The values are the means ± S.D. ($n = 3$). Significantly different from vehicle controls (*, $P < 0.05$) or cells treated with TO-1317 alone (†, $P < 0.05$).

peptide and LXRα but not LXRβ (Fig. 1D). At higher concentrations, RC caused non-specific interference in monitoring fluorescence polarization. No interactions were induced by RF.

3.2. RC and RF compete with synthetic or endogenous ligands for LXR activation

When assayed in the presence of 1 μM TO-1317 (TO-901317), RC and RF reduced the TO-1317-induced association of the SRC-1 peptide with LXRα or LXRβ, indicating the binding of these compounds to the receptors (Fig. 2A). These compounds also decreased LXRα-transactivation elicited by a synthetic LXR agonist TO-1317 (Fig. 2B), although inhibitory effect of RF on LXRβ was insignificant. The ability of RC and RF to compete with endogenous ligands was tested in HepG2 cells. Treatment of the cells with compactin, which has been reported to deplete endogenous ligands for LXR [19,20], led to a 60% reduction in LXRE-dependent transactivation (Fig. 2C). Similarly, RF decreased the luciferase activity to the level of cells treated with compactin. RC had no effect in the absence of compactin but increased luciferase activity by 1.6-fold in compactin-treated cells. RC and RF inhibited the TO-1317-elicited expression of SREBP-1c mRNA in THP-1 cells. RF also decreased the TO-1317-elicited expression in HepG2 cells, although the effect of RC was insignificant (Fig. 2D).

3.3. RC enhances ApoA-I-mediated cellular cholesterol release

We used real-time quantitative PCR to investigate the effect of RC on the expression of LXR target genes, ABCA1, ABCG1, and SREBP-1c, in THP-1 cells. RC (30 μM) increased the ABCA1 mRNA level by 2-fold, while 22RHC (12.5 μM) and TO-1317 (10 nM) caused 2.2- and 2.7-fold inductions, respectively (Fig. 3A). Likewise, RC raised the ABCG1 and SREBP-1c mRNA level by 2.6-fold and 1.6-fold, respectively.

To evaluate whether the increase in ABCA1 mRNA expression was functionally relevant, we examined the effect of RC on cholesterol efflux from THP-1 cells. As shown in Fig. 3B, apoA-I-dependent cholesterol release was increased 2-fold by 10 μM of RC. At 30 μM, this compound also caused a 2-fold elevation in cholesterol release without exogenous apoA-I.

RC had no effect on SREBP-1c and ABCG1 mRNA expression in HepG2 cells, whereas TO-1317 markedly induced expression of both of them (Fig. 3C).

4. Discussion

In the present study, we identified RC as an LXRα-selective agonist. RC bound directly to LXRα and recruited the coacti-

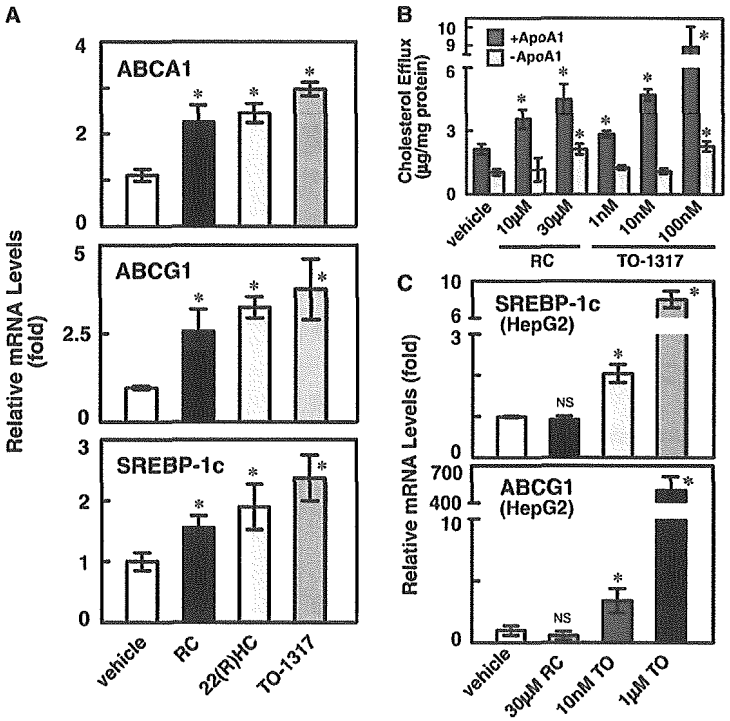

Fig. 3. RC increases ABCA1 and ABCG1 mRNA expression and cellular cholesterol efflux in THP-1 cells without raising SREBP-1c expression in HepG2 cells. (A) THP-1 cells were treated for 24 h with the vehicle (DMSO) alone, RC (30 μM), TO-1317 (10 nM), or 22(*R*)HC (12.5 μM). The levels of ABCA1 and ABCG1 mRNA were measured with TaqMan quantitative real-time PCR analysis. Data were normalized using the 18S rRNA levels and are expressed as the fold induction relative to that in the vehicle-treated cells. The values are the means ± S.D. of three experiments performed in triplicate. (B) Cells were treated for 24 h with the indicated compounds in the presence or absence of apoA-I (10 μg/ml), and the cholesterol released into the medium was analyzed. The values are the means ± S.D. ($n = 3$) of a typical series of three experiments performed. (C) HepG2 cells were treated for 24 h with the vehicle (DMSO) alone, RC (30 μM), or TO-1317 (10 nM or 1 μM). SREBP-1c and ABCG1 mRNA level was measured by quantitative real-time PCR. Data were normalized to 18S rRNA levels and are expressed as the fold induction relative to that in the vehicle-treated cells. The values are the means ± S.D. of three experiments. Statistically significant differences from control are indicated by asterisk (*, $P < 0.05$ and NS, not significant).

vator SRC-1 peptide to the receptor (Fig. 1D), leading to the activation of LXRα-dependent reporter gene transcription (Fig. 1B). RC also possesses the ability to bind to LXRβ. However, its inability to recruit a coactivator to LXRβ (Fig. 1D) resulted in the failure of LXRβ-mediated transactivation. RC was shown to have no ability to activate PPARγ, RARα, RARβ, RARγ, FXR, and RXRα (Fig. 1C).

In contrast to RC, RF was inactive for both LXRα and LXRβ-mediated transactivation (Fig. 1B). This compound was able to bind to LXRα and LXRβ (Fig. 2A) but was unable to promote coactivator association (Fig. 1C). Structural differences between RC and RF suggest that the C-14 hydroxyl group of RC plays a critical role in inducing coactivator association to LXRα, but not to LXRβ, leading to transactivation in a subtype-selective manner.

The competition with the synthetic agonist TO-1317 for the coactivator association (Fig. 2A) and the receptor-mediated transactivation (Fig. 2B) demonstrates that RC functions as an LXRα partial agonist and an LXRβ antagonist. RF functions as an antagonist of LXRα. RF decreased LXRE-dependent luciferase transcription in HepG2 cells to the level of endogenous-ligand depletion by compactin (Fig. 2C), suggesting that endogenous ligand-mediated LXR activation was inhibited by RF. RC increased LXRE-dependent transcription in compactin-treated cells, but not in the absence of compactin. In the intact cells, RC, as well as RF, might compete with endogenous ligands for LXR activation, thereby decreasing endogenous ligand-mediated activation. This latent activity of RC might compensate for this reduction. RC and RF also competed with TO-1317 for SREBP-1c expression in THP-1 cells.

The efflux of cellular cholesterol to HDL constitutes the first stage in the reverse cholesterol transport pathway and plays a critical role in modulating the progression of atherosclerosis [21]. ABCA1 and ABCG1 have been shown to mediate this process [22,23], and LXRα and LXRβ play redundant roles in their expression [9,24]. RC functions as an LXRα partial agonist and LXRβ antagonist. However, RC was shown to raise ABCA1 and ABCG1 mRNA levels and enhance cellular cholesterol efflux in THP-1 cells (Fig. 3A and B). Because human LXRα expression is autoregulated by LXRα itself [25], the stimulation of LXRα may have a stronger effect than that of LXRβ. RC and TO-1317 at higher concentrations increased cholesterol efflux even in the absence of apoA-I. Because THP-1 cells express apoE [26] and ABCA1 at the basal level, increased expression of apoE by LXR activation [27], caveolin-1 [28], or ABCA7 [29] could lead to enhanced cholesterol release, even without apoA-I.

We found that RC did not affect SREBP-1c and ABCG1 expression in hepatoma HepG2 cells (Fig. 3C). This coincides with the apparent inability of RC to enhance LXRE-dependent transactivation in this cell line (Fig. 2C). A possible explanation for this inability is the low LXRα/LXRβ ratio in HepG2 cells. Alternatively, as a partial LXRα agonist/LXRβ antagonist, RC might compete with endogenous ligands produced via the cholesterol synthesis pathway. It is also possible that coactivator-corepressor(s) different from those employed in THP-1 cells might be active in this cell line. Further studies are required to elucidate the precise mechanisms of RC's selective actions. However, because synthetic LXR agonists have been shown to cause hypertriglyceridemia [5], LXR modulators that do not upregulate hepatic lipogenic genes may enable improved therapeutic strategies.

Acknowledgments: This work was supported in part by a grant (MF-16) from the Organization for Pharmaceutical Safety and Research and a grant from the Japan Health Sciences Foundation.

References

[1] Edwards, P.A., Kast, H.R. and Anisfeld, A.M. (2002) BAREing it all: the adoption of LXR and FXR and their roles in lipid homeostasis. J. Lipid Res. 43, 2–12.
[2] Janowski, B.A., Willy, P.J., Devi, T.R., Falck, J.R. and Mangelsdorf, D.J. (1996) An oxysterol signalling pathway mediated by the nuclear receptor LXR alpha. Nature 383, 728–731.
[3] Lehmann, J.M., Kliewer, S.A., Moore, L.B., Smith-Oliver, T.A., Oliver, B.B., Su, J.L., Sundseth, S.S., Winegar, D.A., Blanchard, D.E., Spencer, T.A. and Willson, T.M. (1997) Activation of the nuclear receptor LXR by oxysterols defines a new hormone response pathway. J. Biol. Chem. 272, 3137–3140.
[4] Repa, J.J., Liang, G., Ou, J., Bashmakov, Y., Lobaccaro, J.M., Shimomura, I., Shan, B., Brown, M.S., Goldstein, J.L. and Mangelsdorf, D.J. (2000) Regulation of mouse sterol regulatory element-binding protein-1c gene (SREBP-1c) by oxysterol receptors, LXRalpha and LXRbeta. Genes Dev. 14, 2819–2830.
[5] Schultz, J.R., Tu, H., Luk, A., Repa, J.J., Medina, J.C., Li, L., Schwendner, S., Wang, S., Thoolen, M., Mangelsdorf, D.J., Lustig, K.D. and Shan, B. (2000) Role of LXRs in control of lipogenesis. Genes Dev. 14, 2831–2838.
[6] Yoshikawa, T., Shimano, H., Amemiya-Kudo, M., Yahagi, N., Hasty, A.H., Matsuzaka, T., Okazaki, H., Tamura, Y., Iizuka, Y., Ohashi, K., Osuga, J., Harada, K., Gotoda, T., Kimura, S., Ishibashi, S. and Yamada, N. (2001) Identification of liver X receptor-retinoid X receptor as an activator of the sterol regulatory element-binding protein 1c gene promoter. Mol. Cell Biol. 21, 2991–3000.
[7] Joseph, S.B., Laffitte, B.A., Patel, P.H., Watson, M.A., Matsukuma, K.E., Walczak, R., Collins, J.L., Osborne, T.F. and Tontonoz, P. (2002) Direct and indirect mechanisms for regulation of fatty acid synthase gene expression by liver X receptors. J. Biol. Chem. 277, 11019–11025.
[8] Costet, P., Luo, Y., Wang, N. and Tall, A.R. (2000) Sterol-dependent transactivation of the ABC1 promoter by the liver X receptor/retinoid X receptor. J. Biol. Chem. 275, 28240–28245.
[9] Venkateswaran, A., Repa, J.J., Lobaccaro, J.M., Bronson, A., Mangelsdorf, D.J. and Edwards, P.A. (2000) Human white/murine ABC8 mRNA levels are highly induced in lipid-loaded macrophages. A transcriptional role for specific oxysterols. J. Biol. Chem. 275, 14700–14707.
[10] Lu, T.T., Repa, J.J. and Mangelsdorf, D.J. (2001) Orphan nuclear receptors as eLiXiRs and FiXeRs of sterol metabolism. J. Biol. Chem. 276, 37735–37738.
[11] Alberti, S., Schuster, G., Parini, P., Feltkamp, D., Diczfalusy, U., Rudling, M., Angelin, B., Bjorkhem, I., Pettersson, S. and Gustafsson, J.A. (2001) Hepatic cholesterol metabolism and resistance to dietary cholesterol in LXRbeta-deficient mice. J. Clin. Invest. 107, 565–573.
[12] Peet, D.J., Turley, S.D., Ma, W., Janowski, B.A., Lobaccaro, J.M., Hammer, R.E. and Mangelsdorf, D.J. (1998) Cholesterol and bile acid metabolism are impaired in mice lacking the nuclear oxysterol receptor LXR alpha. Cell 93, 693–704.
[13] Schuster, G.U., Parini, P., Wang, L., Alberti, S., Steffensen, K.R., Hansson, G.K., Angelin, B. and Gustafsson, J.A. (2002) Accumulation of foam cells in liver X receptor-deficient mice. Circulation 106, 1147–1153.
[14] Yoshida, T., Hashimoto, T., Takaoka, S., Kan, Y., Tori, M. and Asakawa, Y. (1996) Phenolic constituents of the liverwort: four novel cyclic Bisbibenzyl dimers from *Blasia pusilla* L. Tetrahedron 52, 14487–14500.
[15] Hashimoto, T., Yoshida, T., Kan, Y., Takaoka, S., Tori, M. and Asakawa, Y. (1994) Structures of four novel macrocyclic Bis(bibenzyl) dimmers, pusilatins A–D from the liverwort *Blasia pusilla*. Tetrahedron Lett. 35, 909–910.
[16] Nishimaki-Mogami, T., Une, M., Fujino, T., Sato, Y., Tamehiro, N., Kawahara, Y., Shudo, K. and Inoue, K. (2004) Identification of intermediates in the bile acid synthetic pathway as ligands for the farnesoid X receptor. J. Lipid Res. 45, 1538–1545.

[17] Fu, X., Menke, J.G., Chen, Y., Zhou, G., MacNaul, K.L., Wright, S.D., Sparrow, C.P. and Lund, E.G. (2001) 27-hydroxycholesterol is an endogenous ligand for liver X receptor in cholesterol-loaded cells. J. Biol. Chem. 276, 38378–38387.
[18] Suzuki, S., Nishimaki-Mogami, T., Tamehiro, N., Inoue, K., Arakawa, R., Abe-Dohmae, S., Tanaka, A.R., Ueda, K. and Yokoyama, S. (2004) Verapamil increases the apolipoprotein-mediated release of cellular cholesterol by induction of ABCA1 expression via Liver X receptor-independent mechanism. Arterioscler. Thromb. Vasc. Biol. 24, 519–525.
[19] DeBose-Boyd, R.A., Ou, J., Goldstein, J.L. and Brown, M.S. (2001) Expression of sterol regulatory element-binding protein 1c (SREBP-1c) mRNA in rat hepatoma cells requires endogenous LXR ligands. Proc. Natl. Acad. Sci. USA 98, 1477–1482.
[20] Wong, J., Quinn, C.M. and Brown, A.J. (2004) Statins inhibit synthesis of an oxysterol ligand for the liver x receptor in human macrophages with consequences for cholesterol flux. Arterioscler. Thromb. Vasc. Biol. 24, 2365–2371.
[21] Joyce, C., Freeman, L., Brewer Jr., H.B. and Santamarina-Fojo, S. (2003) Study of ABCA1 function in transgenic mice. Arterioscler. Thromb. Vasc. Biol. 23, 965–971.
[22] Singaraja, R.R., Brunham, L.R., Visscher, H., Kastelein, J.J. and Hayden, M.R. (2003) Efflux and atherosclerosis: the clinical and biochemical impact of variations in the ABCA1 gene. Arterioscler. Thromb. Vasc. Biol. 23, 1322–1332.
[23] Wang, N., Lan, D., Chen, W., Matsuura, F. and Tall, A.R. (2004) ATP-binding cassette transporters G1 and G4 mediate cellular cholesterol efflux to high-density lipoproteins. Proc. Natl. Acad. Sci. USA 101, 9774–9779.
[24] Repa, J.J., Turley, S.D., Lobaccaro, J.A., Medina, J., Li, L., Lustig, K., Shan, B., Heyman, R.A., Dietschy, J.M. and Mangelsdorf, D.J. (2000) Regulation of absorption and ABC1-mediated efflux of cholesterol by RXR heterodimers. Science 289, 1524–1529.
[25] Laffitte, B.A., Joseph, S.B., Walczak, R., Pei, L., Wilpitz, D.C., Collins, J.L. and Tontonoz, P. (2001) Autoregulation of the human liver X receptor alpha promoter. Mol. Cell Biol. 21, 7558–7568.
[26] Tajima, S., Hayashi, R., Tsuchiya, S., Miyake, Y. and Yamamoto, A. (1985) Cells of a human monocytic leukemia cell line (THP-1) synthesize and secrete apolipoprotein E and lipoprotein lipase. Biochem. Biophys. Res. Commun. 126, 526–531.
[27] Laffitte, B.A., Repa, J.J., Joseph, S.B., Wilpitz, D.C., Kast, H.R., Mangelsdorf, D.J. and Tontonoz, P. (2001) LXRs control lipid-inducible expression of the apolipoprotein E gene in macrophages and adipocytes. Proc. Natl. Acad. Sci. USA 98, 507–512.
[28] Arakawa, R., Abe-Dohmae, S., Asai, M., Ito, J.I. and Yokoyama, S. (2000) Involvement of caveolin-1 in cholesterol enrichment of high density lipoprotein during its assembly by apolipoprotein and THP-1 cells. J. Lipid Res. 41, 1952–1962.
[29] Abe-Dohmae, S., Ikeda, Y., Matsuo, M., Hayashi, M., Okuhira, K., Ueda, K. and Yokoyama, S. (2004) Human ABCA7 supports apolipoprotein-mediated release of cellular cholesterol and phospholipid to generate high density lipoprotein. J. Biol. Chem. 279, 604–611.

Vol 438|15 December 2005|doi:10.1038/nature04223

nature

LETTERS

BDNF from microglia causes the shift in neuronal anion gradient underlying neuropathic pain

Jeffrey A. M. Coull[1,2]*, Simon Beggs[3]*, Dominic Boudreau[1], Dominick Boivin[1], Makoto Tsuda[3,4], Kazuhide Inoue[4], Claude Gravel[5,6], Michael W. Salter[3] & Yves De Koninck[1,2,6]

Neuropathic pain that occurs after peripheral nerve injury depends on the hyperexcitability of neurons in the dorsal horn of the spinal cord[1–3]. Spinal microglia stimulated by ATP contribute to tactile allodynia, a highly debilitating symptom of pain induced by nerve injury[4]. Signalling between microglia and neurons is therefore an essential link in neuropathic pain transmission, but how this signalling occurs is unknown. Here we show that ATP-stimulated microglia cause a depolarizing shift in the anion reversal potential (E_{anion}) in spinal lamina I neurons. This shift inverts the polarity of currents activated by GABA (γ-amino butyric acid), as has been shown to occur after peripheral nerve injury[5]. Applying brain-derived neurotrophic factor (BDNF) mimics the alteration in E_{anion}. Blocking signalling between BDNF and the receptor TrkB reverses the allodynia and the E_{anion} shift that follows both nerve injury and administration of ATP-stimulated microglia. ATP stimulation evokes the release of BDNF from microglia. Preventing BDNF release from microglia by pretreating them with interfering RNA directed against BDNF before ATP stimulation also inhibits the effects of these cells on the withdrawal threshold and E_{anion}. Our results show that ATP-stimulated microglia signal to lamina I neurons, causing a collapse of their transmembrane anion gradient, and that BDNF is a crucial signalling molecule between microglia and neurons. Blocking this microglia–neuron signalling pathway may represent a therapeutic strategy for treating neuropathic pain.

Peripheral nerve injury (PNI)-induced tactile allodynia depends on a depolarizing shift in the E_{anion} of spinal lamina I (LI) neurons in the dorsal spinal cord, causing disinhibition and, in some cases, converting the $GABA_A$-receptor- and glycine-receptor-mediated inhibition to excitation[5]. As microglia are implicated in the induction of neuropathic pain[4], we considered that these glia cells may affect E_{anion} in LI neurons. To investigate this possibility, we administered microglia to the lumbar spinal level of naive rats by an intrathecal catheter as described[4], and subsequently made perforated-patch and whole-cell recordings from LI neurons in acute spinal cord slices prepared from these rats. Prior to slice preparation, we determined the paw withdrawal threshold for each rat[4,5]. Administering control unstimulated microglia produced no change in paw withdrawal threshold, whereas microglia that had been stimulated with ATP caused a progressive decrease in paw withdrawal threshold over the 5 h of testing after injection (Fig. 1a). Cortically and spinally derived microglia produced a comparable decrease in paw withdrawal threshold. Owing to its larger size, the cortex yielded more microglia and was therefore used for all subsequent experiments.

Electrophysiological recordings were made from slices prepared 5 h after intrathecal microglia administration. Using voltage-clamp recording from LI neurons, we found that in spinal slices taken from rats injected with control microglia E_{anion} was -68.3 ± 1.8 mV (mean ± s.e.m; $n = 6$; Fig. 1b). By contrast, in LI neurons from rats that had been administered ATP-stimulated microglia, E_{anion} was -61.6 ± 1.1 mV ($n = 16$, $P < 0.0001$). In addition, using current-clamp recordings, we found that the GABA response switched from hyperpolarizing in control rats to depolarizing in rats treated with ATP-stimulated microglia (Fig. 1c).

We reasoned that, to effect the shift in E_{anion}, ATP-stimulated microglia must signal to the LI dorsal horn neurons. Activated microglia secrete various biologically active signalling molecules, one of which, BDNF[6], has been implicated in the hypersensitivity of dorsal horn neurons that follows sensitization and inflammation[7–9] and in anion gradient shifts in the hippocampus[10]. To test whether BDNF could trigger shifts in pain hypersensitivity and in LI neuronal E_{anion} similar to those resulting from the application of ATP-stimulated microglia, we administered recombinant BDNF intrathecally to naive rats. This locally delivered BDNF produced a significant and transient decrease in paw withdrawal threshold comparable to that produced by ATP-stimulated microglia (Fig. 2a).

To determine whether BDNF could cause a shift in E_{anion}, we bath-applied it to spinal slices taken from naive rats. E_{anion} of LI neurons ($n = 9$) in slices treated with BDNF (>90 min) was significantly less negative than that of LI neurons from control untreated slices ($n = 9$; $P < 0.005$; Fig. 2b). Thus, it seemed possible that responses to GABA might be excitatory, rather than inhibitory, during BDNF administration. We investigated this possibility by monitoring intracellular calcium ($[Ca^{2+}]_i$) after brief applications of GABA in LI neurons ($n = 96$). During perfusion with BDNF and in the presence of glutamate receptor blockers, the proportion of neurons responding to GABA with a rise in $[Ca^{2+}]_i$ increased over time, reaching 31% of neurons recorded between 80 and 120 min ($P < 0.05$; Fig. 2c). The rise in $[Ca^{2+}]_i$ was prevented by the $GABA_A$ receptor blocker bicuculline ($n = 18$; $P < 0.05$), confirming that the effect was mediated by $GABA_A$ receptors. Thus, acute administration of BDNF in slices caused a depolarizing shift in E_{anion} and, in about 30% of the cells, caused GABA to produce net excitation.

To determine the effects of sustained prolonged exposure to BDNF *in vivo*, we administered a BDNF-transducing recombinant adenovirus (adBDNF)[11] intrathecally to the rats ($n = 16$). After injection, adBDNF caused a progressive decrease in paw withdrawal threshold over the 4 d of testing. By contrast, a control adenovirus had no effect

[1]Division de Neurobiologie Cellulaire, Centre de Recherche Université Laval Robert-Giffard, Québec, Québec G1J 2G3, Canada. [2]Department of Pharmacology & Therapeutics, McGill University, Montréal, Québec H3G 1Y6, Canada. [3]Programme in Brain and Behaviour, The Hospital for Sick Children, 555 University Avenue, Toronto, Ontario M5G 1X8, Canada. [4]Department of Molecular and System Pharmacology, Graduate School of Pharmaceutical Sciences, Kyushu University, 3-1-1 Maidashi, Higashi, Fukuoka 812-8582, Japan. [5]Division de Neurobiologie Systémique, Centre de recherche Université Laval Robert-Giffard, Québec, Québec G1J 2G3, Canada. [6]Département de Psychiatrie, Université Laval, Québec, Québec G1K 7P4, Canada.
*These authors contributed equally to this work.

on paw withdrawal threshold over the same period ($n = 6$; $P < 0.005$; Fig. 2d). Because of the prolonged effect of the adBDNF treatment, we could test for changes in E_{anion} in slices taken from treated rats. E_{anion} in LI neurons from adBDNF-injected rats ($n = 7$) was significantly less negative than that in LI neurons from rats treated with the control adenovirus ($n = 4$; $P < 0.01$; Fig. 2e, f). Moreover, GABA application caused some LI neurons from adBDNF-injected rats to fire action potentials (2/7 cells tested), a feature that was not observed in control conditions. Thus, similar to acute administration of BDNF, sustained local release caused a decrease in paw withdrawal threshold, caused a depolarizing shift in E_{anion} and, in some neurons, could switch the action of GABA from inhibitory to excitatory.

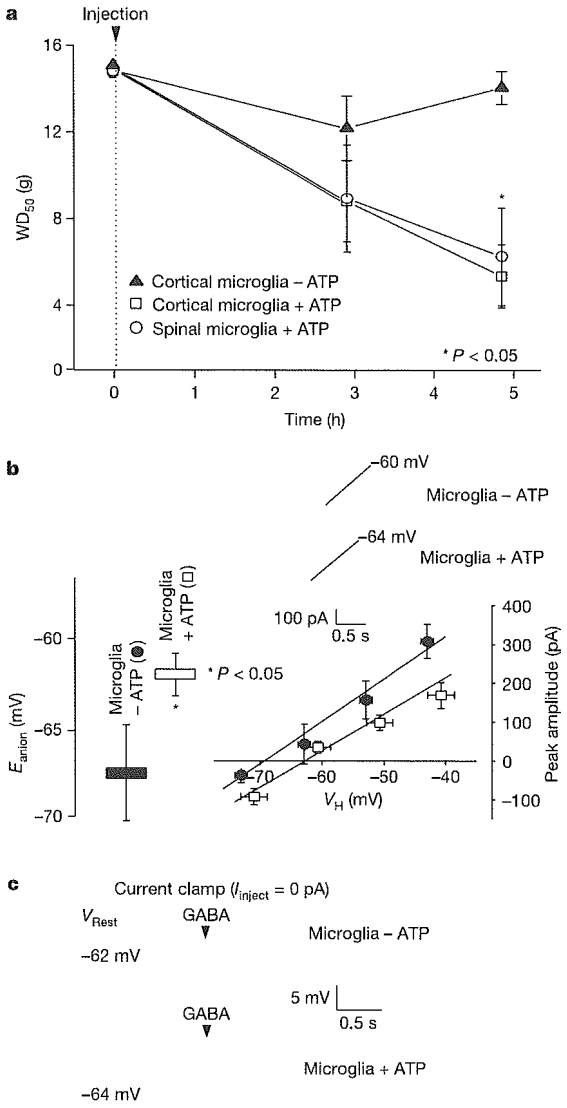

Figure 1 | Spinal delivery of ATP-stimulated microglia to rats evokes allodynia and a depolarizing shift in E_{anion} in spinal LI neurons. a, In naive rats, local spinal delivery of ATP-stimulated microglia (of cortical or spinal origin), but not resting microglia, by means of an intrathecal catheter caused a significant decrease in the mean paw withdrawal threshold (WD_{50}; vertical bars indicate the s.e.m.). **b**, Left, comparison of the mean ± s.e.m. E_{anion} recorded in LI neurons from rats injected with resting or ATP-stimulated microglia. Note that there were no significant changes in the resting membrane potential of the cells. Right, the mean ± s.e.m. peak current evoked by GABA, measured in LI neurons at various values of membrane potential (V_m) in slices taken from the rats in **a**. Horizontal error bars represent interneuron differences. Inset, representative raw traces. **c**, Representative traces in current-clamp recording mode showing that, at resting membrane potential, the postsynaptic response to GABA was depolarizing in a LI neuron taken from a rat with a WD_{50} of 3.4 g, in contrast to the response in a LI neuron taken from a rat with a WD_{50} of 12.6 g, where GABA was hyperpolarizing.

These results show that exogenous BDNF is sufficient to cause tactile allodynia and a shift in E_{anion}, raising the possibility that BDNF might be an endogenous mediator of the sequelae of PNI. To investigate this, we used a function-blocking antibody against the TrkB receptor (anti-TrkB) and a BDNF-sequestering fusion protein (TrkB–Fc), each of which blocks the effects of BDNF[7,9,12,13]. We administered anti-TrkB or TrkB–Fc intrathecally to rats that had developed allodynia 2 weeks after PNI. Both agents acutely reversed the decrease in paw withdrawal threshold ($n = 7$ and $n = 4$, respectively, $P < 0.05$; Fig. 3a). By contrast, vehicle administration to rats with PNI produced no change in withdrawal threshold (data not shown). To determine whether BDNF–TrkB signalling is necessary for the nerve injury-induced shift in E_{anion} in LI neurons, we examined the effect of anti-TrkB applied acutely to spinal cord slices taken from rats with allodynia 2 weeks after PNI. We found that E_{anion} of LI neurons in slices treated with anti-TrkB ($n = 7$) was significantly more negative than E_{anion} in vehicle-treated slices ($n = 6$; $P < 0.05$; Fig. 3b, c). Together, these findings indicate that endogenous BDNF is necessary to sustain both the tactile allodynia and the depolarizing shift in E_{anion} in LI neurons that result from PNI.

If microglia are the source of BDNF, then interfering with BDNF–TrkB signalling should prevent the tactile allodynia and the shift in LI neuronal E_{anion} produced by administering ATP-stimulated microglia (Fig. 4). We tested the first part of this prediction by delivering ATP-stimulated microglia together with either anti-TrkB or TrkB–Fc; the two cocktails produced no change in paw withdrawal threshold over the 5 h after intrathecal injection ($n = 8$ and $n = 7$, respectively; Fig. 4a). By contrast, allodynia developed progressively after the administration of ATP-stimulated microglia without these agents ($n = 8$). Notwithstanding these results, it remained possible that microglia stimulated with ATP might have provoked the release of BDNF from cells in the spinal cord and that the blockers interfered with the action of BDNF from this source rather than from the administered microglia *per se*.

To differentiate between these two possibilities, it was necessary to suppress BDNF production in the microglia that were subsequently stimulated with ATP and then administered intrathecally. We pretreated the cultured microglia with double-stranded short interfering RNA directed against BDNF (BDNF siRNA[14]). The microglia were then stimulated with ATP and, when injected intrathecally into naive rats, did not cause a change in withdrawal threshold ($n = 7$; Fig. 4a). To control for possible nonspecific effects of siRNA, we treated some microglia with a scrambled version of the BDNF siRNA before ATP stimulation; these microglia elicited a robust allodynia ($n = 4$, Fig. 4a). In addition, ATP-evoked Ca^{2+} responses in microglia treated with anti-TrkB or with BDNF siRNA did not differ from those of vehicle-treated control microglia, showing that anti-TrkB or BDNF siRNA treatment did not affect the response of the microglia to ATP (Fig. 4d). Yet, interfering with BDNF–TrkB signalling prevented microglia-induced tactile allodynia.

We then addressed the prediction that the depolarizing shift in E_{anion} produced by ATP-stimulated microglia could be prevented by interfering with BDNF–TrkB signalling. E_{anion} in LI neurons from rats receiving ATP-stimulated microglia together with anti-TrkB or after BDNF siRNA pretreatment did not differ significantly from that in LI neurons from rats receiving unstimulated microglia. However, E_{anion} in LI neurons from either of these groups of rats was significantly more negative than that in LI neurons from rats that had received ATP-stimulated microglia with vehicle (Fig. 4c). Thus, anti-TrkB and BDNF siRNA prevented the shift in E_{anion} induced by ATP-stimulated microglia. Moreover, ATP stimulation ($n = 3$), but

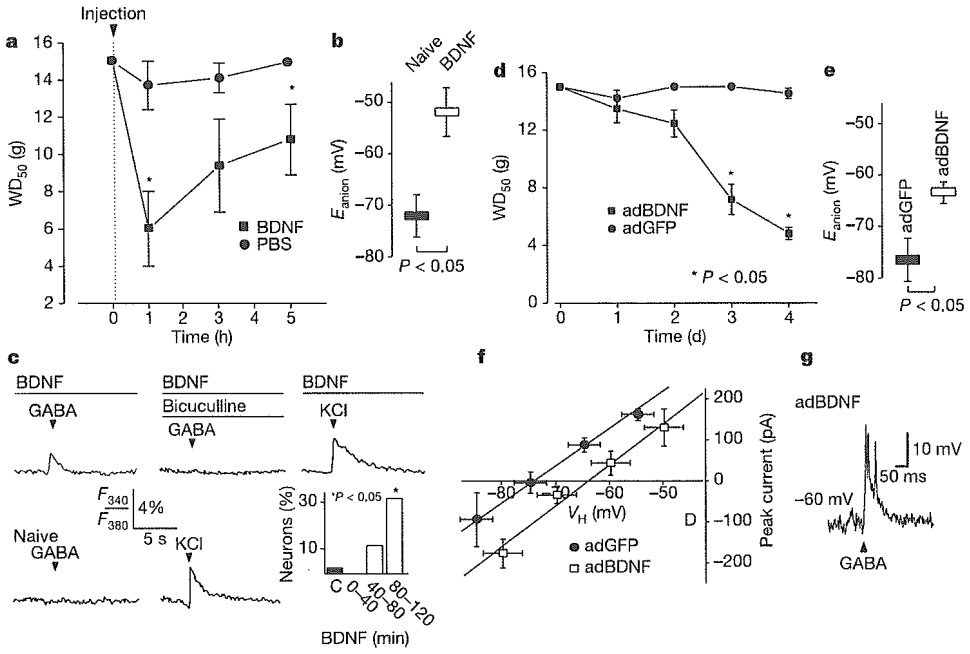

Figure 2 | Enhanced BDNF in the dorsal horn elicits nociceptive hypersensitivity and a depolarizing shift in E_{anion} in spinal LI neurons. **a**, Intrathecal delivery of recombinant human BDNF (20 μg) to the lumbar dorsal horn of intact rats led to a significant and transient decrease in the mean ± s.e.m. WD_{50} within 1 h, as compared with saline control. **b**, Significant depolarization of mean ± s.e.m. E_{anion} in LI neurons in slices treated with BDNF (50 ng ml^{-1}; for >90 min) as compared with slices in control ACSF (Naive). **c**, Representative traces of Ca^{2+} measurements from LI neurons showing that brief GABA application in slices superfused with BDNF caused a bicuculline-sensitive increase in $[Ca^{2+}]_i$. The viability of cells not responding to GABA was confirmed by KCl-mediated responses. Bottom right inset, the proportion of LI neurons showing a GABA-mediated rise in $[Ca^{2+}]_i$ increased progressively, reaching 31% between 80 and 120 min of continuous BDNF perfusion ($\chi^2_{corrected} = 5.15$). By contrast, only 2% of cells responded with a rise in $[Ca^{2+}]_i$ over a similar time period in the absence of BDNF (C; $\chi^2_{corrected} = 6.74$). **d**, Intrathecal administration of adBDNF[11] triggered a delayed and progressive decrease in the mean ± s.e.m. WD_{50} that persisted as long at 4 d after injection. By contrast, administration of a control adenovirus (adGFP) elicited no decrease in WD_{50}. **e**, Significant depolarization of the mean ± s.e.m. E_{anion} in LI neurons in slices taken from the rats in **d**. **f**, Mean ± s.e.m. peak current evoked by GABA measured in LI neurons at various values of V_m in slices taken from the rats in **d**. Horizontal standard error bars represent interneuron differences. **g**, Representative trace in current-clamp recording mode showing that brief GABA application to a LI neuron in a slice taken from an adBDNF-treated rat elicited action potentials.

not vehicle control ($n = 4$), caused release of BDNF from microglia in culture ($P < 0.001$; Fig. 4e). This effect of ATP was blocked by treating the cultures with the P2X receptor blocker TNP-ATP ($n = 3$; $P < 0.05$). In addition, pretreatment of the microglia with BDNF siRNA prevented release of BDNF by ATP stimulation ($n = 3$; $P < 0.001$). Together with our behavioural and electrophysiological results, these findings show that both the decrease in paw withdrawal threshold and the shift in E_{anion} in LI neurons caused by ATP-stimulated microglia require BDNF–TrkB signalling and that the source of BDNF is the microglia themselves.

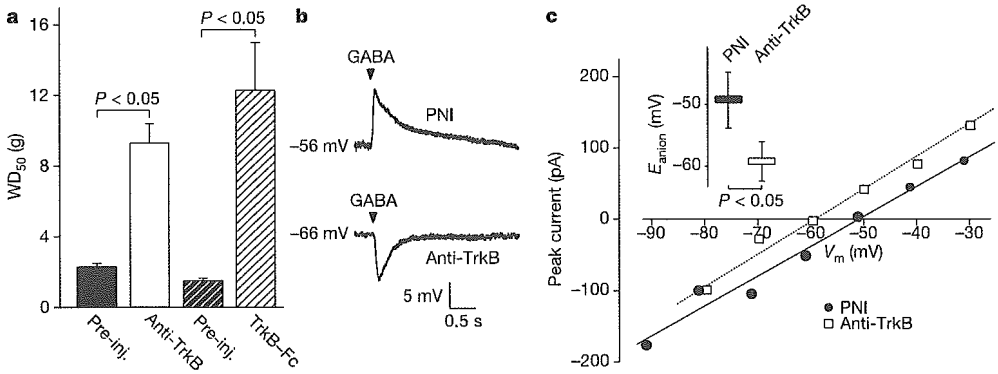

Figure 3 | Functional inhibition of BDNF–TrkB signalling reverses allodynia and the depolarizing shift in E_{anion} in spinal LI neurons in rats with PNI. **a**, Intrathecal administration of either anti-TrkB or TrkB–Fc to the lumbar dorsal horn of rats that showed a robust allodynia in response to PNI caused a significant increase in the mean ± s.e.m. WD_{50}. **b**, Representative traces in current-clamp recording mode showing the postsynaptic response to GABA in LI neurons taken from PNI rats in slices treated with or without anti-TrkB. **c**, Representative current–voltage plots in voltage-clamp recording mode of responses to brief (10-ms) local applications of GABA in two LI neurons in slices taken from PNI rats: one from a slice superfused with control ACSF, the other from a slice after anti-TrkB perfusion (1 μg ml^{-1}). Inset, pooled data showing that anti-TrkB perfusion of slices taken from rats with PNI elicited a significant hyperpolarization of the mean ± s.e.m. E_{anion} in LI neurons.

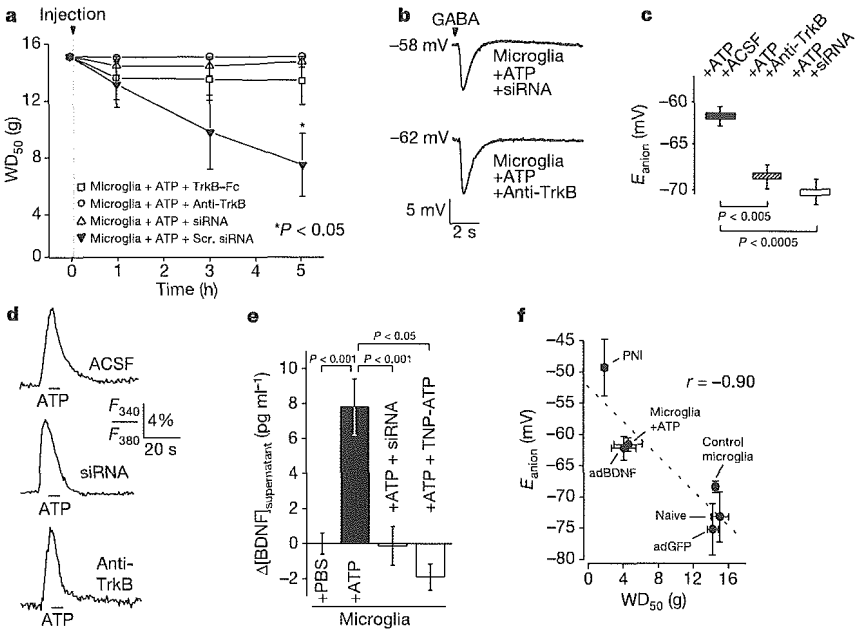

Figure 4 | Microglia-derived BDNF triggers both allodynia and the depolarizing shift in E_{anion} in LI neurons. **a**, Local spinal delivery of ATP-stimulated microglia either incubated with anti-TrkB or TrkB–Fc, or transfected with BDNF siRNA did not cause a significant change in the mean ± s.e.m. WD_{50}. By contrast, ATP-stimulated microglia transfected with a scrambled version of the interfering RNA (Scr. siRNA) caused the WD_{50} to drop significantly after 5 h. **b**, Representative traces in current-clamp recording mode showing postsynaptic responses to GABA in LI neurons from rats treated as in **a**. **c**, Pooled data showing the mean ± s.e.m. E_{anion} measured in LI neurons from rats treated as in **a**. **d**, Representative traces of Ca^{2+} measurements from microglia showing that responses to brief applications of ATP were not affected by exposure of microglia to anti-TrkB or to BDNF siRNA. **e**, ELISA-based measurement of the mean ± s.e.m. BDNF protein in the supernatant of cultured microglia 5 h after treatment with PBS vehicle, ATP, ATP plus TNP-ATP (10 μM) or ATP after pretreatment with BDNF siRNA. **f**, Correlation plot showing the relationship between E_{anion} and WD_{50} (error bars indicate the s.e.m.). The data shown include only those where both WD_{50} and E_{anion} were recorded in the same rat.

Our present findings suggest that, after nerve injury, ATP stimulation of microglia and the subsequent BDNF–TrkB signalling are crucial elements leading to the shift in E_{anion} of LI neurons. We therefore reasoned that inhibiting microglia ATP signalling should suppress the shift in E_{anion} caused by PNI. To test this, we bath-applied TNP-ATP (which reverses nerve-injury-induced tactile allodynia by acting on P2X receptors in microglia[4]) to spinal slices taken from allodynic rats 2 weeks after PNI. In the presence of TNP-ATP, E_{anion} of LI neurons was -59.3 ± 1.8 mV ($n = 6$), which was significantly more negative than that in LI neurons from untreated slices taken from nerve-injured rats (-49.3 ± 4.5 mV; $n = 6$; $P < 0.05$). Thus, P2X receptor activation is necessary to sustain the depolarizing shift in E_{anion} in rats with PNI. Moreover, we found an inverse correlation between paw withdrawal threshold and E_{anion} in LI neurons across all experimental conditions (Fig. 4f), suggesting that E_{anion} is an essential mechanistic link between microglia and allodynia.

Because acutely disrupting the microglia–BDNF–neuron signalling pathway reversed the change in E_{anion} and allodynia, ongoing activation of this pathway must be necessary to maintain nerve-injury-induced pain. Although BDNF has been implicated in spinal nociceptive hypersensitivity, the current framework of thinking on the role of BDNF is based on the hypothesis that the source of this neurotrophin is primary afferent neurons (reviewed in ref. 15). This source of BDNF has been brought into question in neuropathic pain, however, because of evidence indicating that there is a lack of primary-afferent-evoked release of BDNF in the spinal cord after PNI[16]. By showing that BDNF derives from microglia, our findings change the model for understanding how BDNF participates in the nociceptive hypersensitivity that underlies tactile allodynia. Our findings provide a new perspective from which to understand the aetiology of pain hypersensitivity and suggest that targeting microglia-derived BDNF may be a previously unsuspected avenue for treating neuropathic pain.

Our results define a biochemical pathway and a biophysical mechanism by which activated microglia affect neuronal function. Microglia become activated in many pathological processes in the central nervous system[17–20]. Given that depolarizing anion currents can gate plasticity and excitotoxicity[21], the microglia–neuron signalling mechanism that we have identified may be a substrate underlying these pathological disorders.

METHODS

Model of PNI and behavioural studies. PNI was induced as described[5,22]. In brief, a polyethylene cuff (~2 mm in length) was surgically implanted around the sciatic nerve of adult male Sprague–Dawley rats. The 50% paw withdrawal threshold to mechanical stimulation was assessed as described[5,23]. The withdrawal threshold was measured for each rat before use in slice experiments. In this model of PNI, there is microglia activation in the spinal cord ipsilateral to the nerve cuff, as indicated by a considerable increase in labelling for the microglia activation marker OX42 (by anti-CR3/CD11b, Cedarlane; diluted 1:1,000; data not shown).

Slice preparation. Parasagittal slices (300–350 μm) of spinal cord were prepared from ad ult male rats (aged >50 d) as described[24]. Slices were continually superfused (2–3 ml min^{-1}) with artificial cerebrospinal fluid (ACSF) containing (in mM): 126 NaCl, 26 $NaHCO_3$, 10 glucose, 2.5 KCl, 2 $CaCl_2$, 2 $MgCl_2$ and 1.25 NaH_2PO_4 buffer (bubbled with 95% O_2/5% CO_2; pH ≈ 7.4).

Recordings. The pipettes were filled with a solution containing (in mM): 130 potassium methyl sulphate ($KMeSO_4$), 5 CsCl, 2 $MgCl_2$, 11 BAPTA, 1 $CaCl_2$, 4 ATP, 0.4 GTP and 10 HEPES buffer (pH ≈ 7.4). For perforated-patch recordings, 25 μg ml^{-1} gramicidin D, from a stock solution of 10 mg ml^{-1} in dimethylsulphoxide (DMSO), was added to the above solution. GABA was applied locally for 10–50 ms by pressure ejection through a micropipette. Data acquisition and analysis of postsynaptic currents (PSCs) were done as

described[25]. Membrane potential measurements were corrected as described[26]. Neither input resistance nor resting membrane potential of LI neurons was affected significantly by any of the drugs or protocols used in this study. All data are given as the mean ± s.e.m., except where indicated. Statistical significance was tested by using Student's *t*-test for comparison of mean values, χ^2 tests for contingency tables, and mixed-design analyses of variance (*post hoc* Tukey's HSD test) for repeated measures.

Microglia cultures. Rat primary cultures were prepared from neonatal cortex or spinal cord as indicated, under standard conditions as described[4,27], and maintained for 10–14 d in DMEM medium with 10% fetal bovine serum. Microglia were separated from the primary culture by gentle shaking of the flask and were replated on plastic dishes. The cells were removed from the dish surface with a cell scraper and collected in 100 μl of PBS buffer. The density of microglia was measured by using a cell counter, and the volume of PBS was adjusted to give a final density of 1,000 cells per 10 μl. This method produces microglia cultures of >95% purity. For ATP stimulation, the purified microglia were incubated with 50 μM ATP for 1 h.

Intrathecal injections. At least 3 d before drug administration, rats were anaesthetized with sodium pentobarbital (65 mg per kg (body weight)), and a lumbar spinal catheter (PE-10 polyethylene tube) was inserted into the intrathecal space as described[28]. After drug or vehicle administration, rats were killed and their vertebral column was dissected to confirm visually that placement of the catheter was correct. Drugs included BDNF (10 μg per injection), anti-TrkB (30 μg per injection) and TrkB–Fc (5 μg per injection), all of which were prepared in saline plus 10% (v/v) DMSO. For virus-mediated transduction, adenoviral vectors encoding BDNF and enhanced green fluorescent protein (EGFP)[11] were administered once (20 μl, at 2.0×10^{10} plaque-forming units per ml). At the doses used, none of the compounds produced motor disturbances or sedation, as assessed by grasping, righting and placing reflexes and behavioural observations[29]. In all experiments, 30 μl of microglia plus supernatant were injected intrathecally in normal rats, and for all drugs and microglia tested the experimenter was blind to the treatment.

RNA interference. Microglia cultures were transfected with siRNA directed against BDNF or scrambled siRNA (Dharmacon) with Lipofectamine 2000 (Invitrogen) according to the manufacturer's instructions. In brief, siRNA and Lipofectamine were diluted in serum-free medium, mixed and added to the microglia cultures. Transfection was allowed to occur for 5 h and the microglia were collected as described above for subsequent stimulation and intrathecal injection. The BDNF siRNA consisted of four pooled 21-nucleotide duplexes. The sequences of the four duplexes[14] were TCGAAGAGCTGCTGGATGA, TATGTACACTGACCATTAA, GAGCGTGTGTGACAGTATT and GAACTACCC AATCGTATGT.

Enzyme-linked immunosorbent assay. To measure BDNF secretion, we prepared microglia under the various experimental conditions described above and incubated them at 37 °C for 6 h to model the above *in vivo* experiments. Supernatants were removed and BDNF protein concentration was measured by ELISA (Chemicon).

Calcium imaging. Spinal cord slices were prepared for Ca^{2+} imaging and tested for responses to GABA as described[5]. Primary cultures of microglia were prepared as above, transferred to standard coverslips and incubated with 2.5 μM Fura-2-AM in HEPES-buffered saline plus 0.01% DMSO for 45 min. After fluorophore loading, changes in $[Ca^{2+}]_i$ in individual microglia were evoked with brief (~5 s) applications of ATP (10 μM) from a micropipette. $[Ca^{2+}]_i$ was fluorometrically measured with a 40× water-immersion objective on a Zeiss Axioscope equipped with epifluorescence optics. Images were acquired by using a TILL Photonics monochromator coupled to a CCD camera, and regions of interest (for ratio analysis) were drawn on clearly distinct cell bodies.

Received 13 June; accepted 8 September 2005.

1. Woolf, C. J. & Salter, M. W. Neuronal plasticity: increasing the gain in pain. *Science* **288**, 1765–1769 (2000).
2. Ji, R. R. & Strichartz, G. Cell signalling and the genesis of neuropathic pain. *Sci. STKE* 2004, reE14 (2004).
3. Lewin, G. R., Lu, Y. & Park, T. J. A plethora of painful molecules. *Curr. Opin. Neurobiol.* 14, 443–449 (2004).
4. Tsuda, M. *et al.* P2X4 receptors induced in spinal microglia gate tactile allodynia after nerve injury. *Nature* **424**, 778–783 (2003).
5. Coull, J. A. *et al.* *Trans*-synaptic shift in anion gradient in spinal lamina I neurons as a mechanism of neuropathic pain. *Nature* **424**, 938–942 (2003).
6. Nakajima, K., Tohyama, Y., Kohsaka, S. & Kurihara, T. Ceramide activates microglia to enhance the production/secretion of brain-derived neurotrophic factor (BDNF) without induction of deleterious factors *in vitro*. *J. Neurochem.* **80**, 697–705 (2002).
7. Mannion, R. J. *et al.* Neurotrophins: peripherally and centrally acting modulators of tactile stimulus-induced inflammatory pain hypersensitivity. *Proc. Natl Acad. Sci. USA* **96**, 9385–9390 (1999).
8. Heppenstall, P. A. & Lewin, G. R. BDNF but not NT-4 is required for normal flexion reflex plasticity and function. *Proc. Natl Acad. Sci. USA* **98**, 8107–8112 (2001).
9. Thompson, S. W., Bennett, D. L., Kerr, B. J., Bradbury, E. J. & McMahon, S. B. Brain-derived neurotrophic factor is an endogenous modulator of nociceptive responses in the spinal cord. *Proc. Natl Acad. Sci. USA* **96**, 7714–7718 (1999).
10. Rivera, C. *et al.* BDNF-induced TrkB activation down-regulates the K^+–Cl^- cotransporter KCC2 and impairs neuronal Cl^- extrusion. *J. Cell Biol.* **159**, 747–752 (2002).
11. Gravel, C., Gotz, R., Lorrain, A. & Sendtner, M. Adenoviral gene transfer of ciliary neurotrophic factor and brain-derived neurotrophic factor leads to long-term survival of axotomized motor neurons. *Nature Med.* **3**, 765–770 (1997).
12. Balkowiec, A. & Katz, D. M. Activity-dependent release of endogenous brain-derived neurotrophic factor from primary sensory neurons detected by ELISA *in situ*. *J. Neurosci.* **20**, 7417–7423 (2000).
13. Jiang, B., Akaneya, Y., Hata, Y. & Tsumoto, T. Long-term depression is not induced by low-frequency stimulation in rat visual cortex *in vivo*: a possible preventing role of endogenous brain-derived neurotrophic factor. *J. Neurosci.* **23**, 3761–3770 (2003).
14. Baker-Herman, T. L. *et al.* BDNF is necessary and sufficient for spinal respiratory plasticity following intermittent hypoxia. *Nature Neurosci.* **7**, 48–55 (2004).
15. Malcangio, M. & Lessmann, V. A common thread for pain and memory synapses? Brain-derived neurotrophic factor and trkB receptors. *Trends Pharmacol. Sci.* **24**, 116–121 (2003).
16. Lever, I., Cunningham, J., Grist, J., Yip, P. K. & Malcangio, M. Release of BDNF and GABA in the dorsal horn of neuropathic rats. *Eur. J. Neurosci.* **18**, 1169–1174 (2003).
17. Nguyen, M. D., Julien, J. P. & Rivest, S. Innate immunity: the missing link in neuroprotection and neurodegeneration? *Nature Rev. Neurosci* **3**, 216–227 (2002).
18. Streit, W. J., Walter, S. A. & Pennell, N. A. Reactive microgliosis. *Prog. Neurobiol.* **57**, 563–581 (1999).
19. Kreutzberg, G. W. Microglia: a sensor for pathological events in the CNS. *Trends Neurosci.* **19**, 312–318 (1996).
20. Gonzalez-Scarano, F. & Baltuch, G. Microglia as mediators of inflammatory and degenerative diseases. *Annu. Rev. Neurosci.* **22**, 219–240 (1999).
21. Staley, K. J., Soldo, B. L. & Proctor, W. R. Ionic mechanisms of neuronal excitation by inhibitory $GABA_A$ receptors. *Science* **269**, 977–981 (1995).
22. Mosconi, T. & Kruger, L. Fixed-diameter polyethylene cuffs applied to the rat sciatic nerve induce a painful neuropathy: ultrastructural morphometric analysis of axonal alterations. *Pain* **64**, 37–57 (1996).
23. Chaplan, S. R., Bach, F. W., Pogrel, J. W., Chung, J. M. & Yaksh, T. L. Quantitative assessment of tactile allodynia in the rat paw. *J. Neurosci. Methods* **53**, 55–63 (1994).
24. Chery, N., Yu, X. H. & De Koninck, Y. Visualization of lamina I of the dorsal horn in live adult rat spinal cord slices. *J. Neurosci. Methods* **96**, 133–142 (2000).
25. Keller, A. F., Coull, J. A., Chery, N., Poisbeau, P. & De Koninck, Y. Region-specific developmental specialization of GABA–glycine cosynapses in laminas I-II of the rat spinal dorsal horn. *J. Neurosci.* **21**, 7871–7880 (2001).
26. Tyzio, R. *et al.* Membrane potential of CA3 hippocampal pyramidal cells during postnatal development. *J. Neurophysiol.* **90**, 2964–2972 (2003).
27. Nakajima, K. *et al.* Identification of elastase as a secretory protease from cultured rat microglia. *J. Neurochem.* **58**, 1401–1408 (1992).
28. Yaksh, T. L., Jessell, T. M., Gamse, R., Mudge, A. W. & Leeman, S. E. Intrathecal morphine inhibits substance P release from mammalian spinal cord *in vivo*. *Nature* **286**, 155–157 (1980).
29. Coderre, T. J. & Van Empel, I. The utility of excitatory amino acid (EAA) antagonists as analgesic agents I. Comparison of the antinociceptive activity of various classes of EAA antagonists in mechanical, thermal and chemical nociceptive tests. *Pain* **59**, 345–352 (1994).

Acknowledgements We thank F. Nault for technical assistance; J. Zhang for conducting OX42 immunostaining; and P. De Koninck, M. Cordero-Erausquin, F. Keller and C. Labrakakis for discussions on the manuscript. This work was supported by Canadian Institutes of Health Research (CIHR) grants (to Y.D.K. and to M.W.S.), Brain Repair Program of Neuroscience Canada and its partner the Ontario Neurotrauma Foundation through the BRP. J.A.M.C. was the recipient of a doctoral award from the CIHR; Y.D.K. is a Senior Scholar of the Fonds de la recherche en santé du Québec (FRSQ); S.B. was the recipient of a fellowship from a Strategic Training Program Grant from the CIHR.

Author Information Reprints and permissions information is available at npg.nature.com/reprintsandpermissions. The authors declare no competing financial interests. Correspondence and requests for materials should be addressed to Y.D.K. (Yves.DeKoninck@crulrg.ulaval.ca) or M.W.S. (mike.salter@utoronto.ca).